Research Article

Carsten Carstensen, Asha K. Dond and Hella Rabus*

Quasi-Optimality of Adaptive Mixed FEMs for Non-selfadjoint Indefinite Second-Order Linear Elliptic Problems

https://doi.org/10.1515/cmam-2019-0034
Received December 13, 2018; accepted December 20, 2018

Abstract: The well-posedness and the a priori and a posteriori error analysis of the lowest-order Raviart–Thomas mixed finite element method (MFEM) has been established for non-selfadjoint indefinite second-order linear elliptic problems recently in an article by Carstensen, Dond, Nataraj and Pani (*Numer. Math.*, 2016). The associated adaptive mesh-refinement strategy faces the difficulty of the flux error control in $H(\mathrm{div}, \Omega)$ and so involves a data-approximation error $\|f - \Pi_0 f\|$ in the L^2 norm of the right-hand side f and its piecewise constant approximation $\Pi_0 f$. The separate marking strategy has recently been suggested with a split of a Dörfler marking for the remaining error estimator and an optimal data approximation strategy for the appropriate treatment of $\|f - \Pi_0 f\|_{L^2(\Omega)}$. The resulting strategy presented in this paper utilizes the abstract algorithm and convergence analysis of Carstensen and Rabus (*SINUM*, 2017) and generalizes it to general second-order elliptic linear PDEs. The argument for the treatment of the piecewise constant displacement approximation u_{RT} is its supercloseness to the piecewise constant approximation $\Pi_0 u$ of the exact displacement u. The overall convergence analysis then indeed follows the axioms of adaptivity for separate marking. Some results on mixed and nonconforming finite element approximations on the multiply connected polygonal 2D Lipschitz domain are of general interest.

Keywords: Adaptivity, Separate Marking, Finite Element Method, Mixed Finite Element Method, Optimal Convergence, Axioms of Adaptivity, General Second-order Linear Elliptic Problems

MSC 2010: 65N12, 65N15, 65N30, 65N50, 65Y20

Dedicated to Amiya K. Pani on the occasion of his 60th birthday and part of the special issue "Recent Advances in PDE: Theory, Computations and Applications" in his honour.

1 Introduction

The convergence analysis of adaptive mixed finite element methods (AMFEM) stated in [6–8, 11] for the Laplacian is completed in this paper for non-selfadjoint indefinite second-order linear elliptic problems via separate marking with the axioms from [8]. Given a right-hand side $f \in L^2(\Omega)$ and piecewise constant coefficients in a (possibly multiply connected) bounded polygonal Lipschitz domain $\Omega \subset \mathbb{R}^2$, the general second-order linear elliptic PDE seeks $u \in H^1_0(\Omega)$ such that

$$\mathcal{L}\, u := -\mathrm{div}(\mathbf{A}\nabla u + u\mathbf{b}) + \gamma u = f \quad \text{in } \Omega. \tag{1.1}$$

***Corresponding author: Hella Rabus,** Institut für Mathematik, Humboldt-Universität zu Berlin, 10099 Berlin, Germany, e-mail: rabus@math.hu-berlin.de
Carsten Carstensen, Institut für Mathematik, Humboldt-Universität zu Berlin, 10099 Berlin, Germany, e-mail: cc@math.hu-berlin.de
Asha K. Dond, Department of Mathematics, Indian Institute of Science, Bangalore, India, e-mail: asha16@math.iisc.ernet.in

The coefficients $\mathbf{A}$, $\mathbf{b}$, and γ are all piecewise constant functions and the symmetric matrix $\mathbf{A}$ is assumed to be positive definite with universal positive eigenvalue bounds from below and above. The entire paper solely assumes that $\mathcal{L} : H^1_0(\Omega) \to H^{-1}(\Omega)$ is injective (i.e., has a trivial kernel); then it is bijective with a bounded inverse and satisfies a global inf-sup condition. The flux variable $\mathbf{p} = -(\mathbf{A}\nabla u + u\mathbf{b})$ with $\mathbf{b}^\star = \mathbf{A}^{-1}\mathbf{b}$ allows to recast problem (1.1) as a first-order system: Seek $u \in H^1_0(\Omega)$ such that

$$\mathbf{A}^{-1}\mathbf{p} + u\mathbf{b}^\star + \nabla u = 0 \quad \text{and} \quad \operatorname{div}\mathbf{p} + \gamma u = f \quad \text{in } \Omega. \tag{1.2}$$

The mixed formulation of (1.1) seeks $(\mathbf{p}, u) \in H(\operatorname{div}, \Omega) \times L^2(\Omega)$ such that

$$\begin{aligned} (\mathbf{A}^{-1}\mathbf{p} + u\mathbf{b}^\star, \mathbf{q})_{L^2(\Omega)} - (\operatorname{div}\mathbf{q}, u)_{L^2(\Omega)} &= 0, \\ (\operatorname{div}\mathbf{p}, v)_{L^2(\Omega)} + (\gamma u, v)_{L^2(\Omega)} &= (f, v)_{L^2(\Omega)} \end{aligned} \tag{1.3}$$

for all $\mathbf{q} \in H(\operatorname{div}, \Omega)$ and for all $v \in L^2(\Omega)$. The well-posedness of (1.3) has been studied in [4, Theorem 2.1] using the equivalence of the weak formulation of (1.1) and the mixed formulation (1.3). The mixed finite element discretization of (1.3) utilizes the piecewise constant functions $P_0(\mathcal{T})$ on $\mathcal{T}$ and the lowest-order Raviart–Thomas finite element space $\mathrm{RT}_0(\mathcal{T}) \subset H(\operatorname{div}, \Omega)$ and seeks $(\mathbf{p}_{\mathrm{RT}}, u_{\mathrm{RT}}) \in \mathrm{RT}_0(\mathcal{T}) \times P_0(\mathcal{T})$ such that

$$\begin{aligned} (\mathbf{A}^{-1}\mathbf{p}_{\mathrm{RT}} + u_{\mathrm{RT}}\mathbf{b}^\star, \mathbf{q}_{\mathrm{RT}})_{L^2(\Omega)} - (\operatorname{div}\mathbf{q}_{\mathrm{RT}}, u_{\mathrm{RT}})_{L^2(\Omega)} &= 0, \\ (\operatorname{div}\mathbf{p}_{\mathrm{RT}}, v_{\mathrm{RT}})_{L^2(\Omega)} + (\gamma u_{\mathrm{RT}}, v_{\mathrm{RT}})_{L^2(\Omega)} &= (\Pi_0 f, v_{\mathrm{RT}})_{L^2(\Omega)} \end{aligned} \tag{1.4}$$

for all $\mathbf{q}_{\mathrm{RT}} \in \mathrm{RT}_0(\mathcal{T})$ and for all $v_{\mathrm{RT}} \in P_0(\mathcal{T})$. The well-posedness of (1.4) has been established in [4, Theorem 4.2] under the additional assumption that the initial mesh-size is sufficiently small.

The convergence and quasi-optimality of adaptive finite element methods for linear symmetric elliptic problems has been discussed in the literature [1, 2, 5, 7–9, 17, 18, 20, 21] and the references mentioned therein. For the non-symmetric case $\mathbf{b} \neq 0$ and for adaptive conforming FEMs, the optimal convergence rates have been established in [15] with a collective marking strategy based on a posteriori error estimation, and – in contrast to the results in [16] – without the interior node property for the refinement. The convergence of adaptive nonconforming FEMs for the non-symmetric and indefinite problem has been derived in [10] with a different separate marking strategy. The adaptive mixed FEM (1.4) has been considered in [13] with a combined norm of the L^2 norm in the flux error and the L^2 norm in the displacement error. Their quasi-optimality analysis is based on some nonstandard adaptive separate marking scheme and a special relation between the mixed FEM and nonconforming schemes.

This paper develops the quasi-optimality of adaptive MFEMs with the natural $H(\operatorname{div})$ norm, that is, the combination of a flux error in the $H(\operatorname{div})$ norm and the displacement error in the L^2 norm via the axioms for separate marking from [8]. The total adaptive estimator is the sum of the residual-based error estimator $\eta(\mathcal{T})$ and the data approximation error $\mu(\mathcal{T})$. Given a parameter $\kappa > 0$, the separate marking scheme runs either the Dörfler marking [14] on $\eta(\mathcal{T})$ if $\mu^2(\mathcal{T}) \leq \kappa\eta^2(\mathcal{T})$ or an optimal data approximation algorithm as in [7, 17, 18] to reduce $\mu(\mathcal{T})$. The main challenge is the proof of the axioms of discrete reliability and quasi-orthogonality for the non-symmetric mixed problem.

The first intermediate solution concerns the discrete flux approximation with a prescribed divergence on the coarse triangulation in the finer Raviart–Thomas space and a generalization of the corresponding design from [7, 8, 11]. The second intermediate solution is the integral mean $\Pi_0 u$ of the exact displacement u and its supercloseness

$$\|\Pi_0 u - u_{\mathrm{RT}}\| \leq C h_{\max}^{\alpha}(\|\mathbf{p} - \mathbf{p}_{\mathrm{RT}}\|_{H(\operatorname{div},\Omega)} + \|u - u_{\mathrm{RT}}\|) \tag{1.5}$$

in the proof of quasi-orthogonality (A4$_\epsilon$) below. In fact, this difficulty does not arise in [8] for $\mathbf{b} \equiv 0$. At first glance, the extended Marini-type identity [4, equation (4.3)] states that u_{CR} is close to $\Pi_0 u_{\mathrm{CR}}$ for some associated Crouzeix–Raviart solution u_{CR}, which is superclose to u by L^2-duality arguments with $\alpha > 0$ from reduced elliptic regularity. This argument, however, leads to (1.5) up to an additional term $\|h_{\mathcal{T}} \operatorname{div}\mathbf{p}_{\mathrm{RT}}\|$, which is *not* included in the error estimator η utilized in this paper. In fact, η solely involves the term $\|h^2_{\mathcal{T}} \operatorname{div}\mathbf{p}_{\mathrm{RT}}\|$ with a higher power of the localized mesh-size $h_{\mathcal{T}}$.

The remaining parts of the paper are organized as follows. Section 2 establishes the notation, the a posteriori error estimators, the adaptive algorithm with separate marking (Safem), and recalls the axioms of adaptivity (A1)–(A4), (B1)–(B2), and quasimonotonicity (QM) with the optimal convergence rates from [8]. Section 3 starts with the proof of stability (A1) and reduction (A2) for the error estimators and distance

functions at hand. Section 4 is devoted to the discrete reliability based on a discrete Helmholtz decomposition in 2D for multiply connected domains. Section 5 verifies the quasi-orthogonality based on (1.5) with a direct proof in Lemma 5.1. Numerical experiments in Section 6 investigate the condition on sufficiently small parameters such as the bulk parameter and the mesh-size for optimal convergence rates.

The presentation is laid out for two-dimensional polygonal domains and the lowest-order case. The coefficients are assumed piecewise constant for simplicity to avoid extra perturbation terms as in [9]. The generalization to 3D may follow the lines of this paper and replaces the discrete Helmholtz decomposition as in [7] for a simply connected domain. The analysis of higher-order finite element approximations requires a new argument for the stability of the discrete problems in that [4] and part of the proofs in this paper utilize the equivalence to the Crouzeix–Raviart nonconforming FEM, which is open in 3D for higher polynomial degrees.

Standard notation on Lebesgue and Sobolev spaces such as $L^2(\Omega)$, $H^1_0(\Omega)$, and $H(\mathrm{div},\Omega)$ and their norms with $\|\bullet\| := \|\bullet\|_{L^2(\Omega)}$ and $\|\bullet\|_\infty := \|\bullet\|_{L^\infty(\Omega)}$ apply throughout the paper. The notation $A \lesssim B$ abbreviates $A \le CB$ for a mesh-size independent generic constant $C > 0$, which may depend on the domain Ω and the shape but not the size of the triangles of the corresponding shape-regular triangulation. The constant C may also depend on the coefficients $\mathbf{A}$, $\mathbf{b}$, and γ through lower and upper bounds of the positive eigenvalues of $\mathbf{A}$ and the upper bound $\|\mathbf{b}\|_\infty + \|\gamma\|_\infty$ for the remaining coefficients. Furthermore, $A \approx B$ abbreviates $A \lesssim B$ and $B \lesssim A$. The context depending symbol $|\bullet|$ denotes the area of a domain, the length of an edge, the counting measure (cardinality) of a set, the absolute value of a real number, or the Euclidean length of a vector.

2 Preliminaries

This section first introduces the necessary notation for the definition and analysis of adaptive algorithms with separate marking. The axioms of adaptivity from [8] are slightly simplified to match the setting of this paper.

2.1 Notation

Let $\mathcal{T}$ be an admissible triangulation of the bounded polygonal domain Ω and let $\mathbb{T}(\mathcal{T})$ be the set of all admissible triangulations refined from $\mathcal{T}$ by newest vertex bisection [20]. Let $\mathcal{E}(T)$ denote the set of the three edges of a triangle $T \in \mathcal{T}$, let $\mathcal{E}$ (resp. $\mathcal{E}(\Omega)$ and $\mathcal{E}(\partial\Omega)$) denote the set of all (resp. interior and boundary) edges in the triangulation $\mathcal{T}$ and let $\mathcal{N}$ be the set of its vertices.

Let $h_{\max} := \max_{T\in\mathcal{T}} h_T$ denote the maximal local mesh-size $h_T := |T|^{\frac{1}{2}}$ and let ν_E and τ_E are the unit normal and tangential vectors along $E \in \mathcal{E}(T)$ of $T \in \mathcal{T}$. The jump $[\mathbf{q}]_E := \mathbf{q}|_{T_+} - \mathbf{q}|_{T_-}$ of $\mathbf{q}$ is defined across an interior edge E shared by the two triangles T_+ and T_-, which form the edge patch $\overline{\omega_E}$. For any boundary edge $E \in \partial\Omega$, let $\omega_E = T_+$ denote the interior of the triangle $T_+ = \overline{\omega_E}$ with the edge $E \in \mathcal{E}(\overline{\omega_E})$ and the jump $[\,\cdot\,]_E$ reduces to the trace (that is, the exterior jump contribution vanishes according to the homogeneous boundary condition). For $v \in H^1(\Omega;\mathbb{R})$ and $\Phi := (\phi_1,\phi_2) \in H^1(\Omega;\mathbb{R}^2)$, the curl and gradient operators read

$$\mathrm{Curl}\, v = \Big(-\frac{\partial v}{\partial y}, \frac{\partial v}{\partial x}\Big), \quad \mathrm{curl}\,\Phi = \frac{\partial \phi_1}{\partial y} - \frac{\partial \phi_2}{\partial x}, \quad \nabla v = \Big(\frac{\partial v}{\partial x}, \frac{\partial v}{\partial y}\Big).$$

The piecewise gradient ∇_{NC} acts as $(\nabla_{\mathrm{NC}} v)|_T = \nabla(v|_T)$ for all $T \in \mathcal{T}$. Let P_r denote the algebraic polynomials of degree at most r and set

$$P_r(\mathcal{T}) := \{v \in L^2(\Omega) : v|_T \in P_r(T) \text{ for all } T \in \mathcal{T}\}, \quad S^1(\mathcal{T}) := P_1(\mathcal{T}) \cap C(\Omega).$$

Let Π_0 denote the piecewise L^2 projection onto $P_0(\mathcal{T})$ with respect to the shape-regular triangulation $\mathcal{T}$. The associated nonconforming Crouzeix–Raviart and lowest-order Raviart–Thomas mixed finite element spaces read

$$\mathrm{CR}^1(\mathcal{T}) := \{v \in P_1(\mathcal{T}) : v \text{ is continuous in all midpoints } \mathrm{mid}(E) \text{ of edges } E \in \mathcal{E}\},$$
$$\mathrm{CR}^1_0(\mathcal{T}) := \{v \in \mathrm{CR}^1(\mathcal{T}) : v(\mathrm{mid}(E)) = 0 \text{ for all } E \in \mathcal{E}(\partial\Omega)\},$$
$$\mathrm{RT}_0(\mathcal{T}) := \{\mathbf{q} \in H(\mathrm{div},\Omega) : \forall T \in \mathcal{T}\ \exists \mathbf{c} \in \mathbb{R}^2\ \exists d \in \mathbb{R}\ \forall \mathbf{x} \in T,\ \mathbf{q}(\mathbf{x}) = \mathbf{c} + d\mathbf{x}\}.$$

2.2 A Posteriori Error Control

The a posteriori error control for problem (1.4) has been established in [4, Theorem 5.5]: Given the unique solutions $(\mathbf{p}, u)$ to (1.3) and $(\mathbf{p}_{\mathrm{RT}}, u_{\mathrm{RT}})$ to (1.4), for small initial mesh-size h_0, the equivalence

$$\|\mathbf{p} - \mathbf{p}_{\mathrm{RT}}\|^2_{H(\mathrm{div},\Omega)} + \|u - u_{\mathrm{RT}}\|^2 \approx \sigma^2(\mathcal{T}) := \eta^2(\mathcal{T}) + \mu^2(\mathcal{T}) \tag{2.1}$$

holds for the (squared) error estimator $\eta(\mathcal{T})$ and data approximation $\mu(\mathcal{T})$ defined by

$$\begin{aligned} \eta^2(\mathcal{T}) &:= \sum_{T\in\mathcal{T}} \eta^2(\mathcal{T}, T) \quad \text{with} \\ \eta^2(\mathcal{T}, T) &:= |T|^{\frac{1}{2}} \sum_{E\in\mathcal{E}(T)} \|[\mathbf{A}^{-1}\mathbf{p}_{\mathrm{RT}} + u_{\mathrm{RT}}\mathbf{b}^\star]_E \cdot \tau_E\|^2_{L^2(E)} + |T|\|\mathbf{A}^{-1}\mathbf{p}_{\mathrm{RT}} + u_{\mathrm{RT}}\mathbf{b}^\star\|^2_{L^2(T)} \end{aligned} \tag{2.2}$$

and

$$\mu^2(\mathcal{T}) := \sum_{T\in\mathcal{T}} \mu^2(T) \quad \text{with } \mu^2(T) := \|f - \Pi_0 f\|^2_{L^2(T)}. \tag{2.3}$$

Given the discrete solution $(\mathbf{p}_{\mathrm{RT}}, u_{\mathrm{RT}})$ and $(\widehat{\mathbf{p}_{\mathrm{RT}}}, \widehat{u_{\mathrm{RT}}})$ with respect to the admissible triangulation $\mathcal{T}$ and its refinement $\widehat{\mathcal{T}} \in \mathbb{T}(\mathcal{T})$, respectively, the distance function reads

$$\delta^2(\mathcal{T}, \widehat{\mathcal{T}}) := \|\widehat{\mathbf{p}_{\mathrm{RT}}} - \mathbf{p}_{\mathrm{RT}}\|^2_{H(\mathrm{div},\Omega)} + \|\widehat{u_{\mathrm{RT}}} - u_{\mathrm{RT}}\|^2 \tag{2.4}$$

with the weighted norm from

$$\|\widehat{\mathbf{p}_{\mathrm{RT}}} - \mathbf{p}_{\mathrm{RT}}\|^2_{H(\mathrm{div},\Omega)} := \|\mathbf{A}^{-\frac{1}{2}}(\widehat{\mathbf{p}_{\mathrm{RT}}} - \mathbf{p}_{\mathrm{RT}})\|^2 + \|\mathrm{div}(\widehat{\mathbf{p}_{\mathrm{RT}}} - \mathbf{p}_{\mathrm{RT}})\|^2.$$

2.3 SAFEM – The Adaptive Algorithm with Separate Marking

The separate marking scheme runs two alternatives A and B depending on the ratio of η_ℓ and μ_ℓ and some small positive input parameters θ_A and κ.

Algorithm 1. SAFEM$(\theta_A, \rho_B, \kappa, \mathcal{T}_0)$.

Input: $\mathcal{T}_0$ with maximal mesh-size h_0, $0 < \theta_A < 1$, $0 < \rho_B < 1$, $0 < \kappa$.

for $\ell = 0, 1, \ldots$

- COMPUTE indicators $\eta^2_\ell(T) := \eta^2(\mathcal{T}_\ell, T)$, $\mu^2(T)$ for $T \in \mathcal{T}_\ell$ by (2.2)–(2.3).
- **if** $\mu^2_\ell := \mu^2(\mathcal{T}_\ell) \le \kappa\eta^2_\ell$ `// Case (A)`
  - SELECT a subset $\mathcal{M}_\ell \subseteq \mathcal{T}_\ell$ of (almost) minimal cardinality with
$$\theta_A \eta^2_\ell \le \eta^2_\ell(\mathcal{M}_\ell) := \sum_{T\in\mathcal{M}_\ell} \eta^2_\ell(T).$$
  - RUN $\mathcal{T}_{\ell+1} :=$ REFINE$(\mathcal{T}_\ell, \mathcal{M}_\ell)$.
- **else** `// Case (B)`
  - RUN $\mathcal{T} =$ `approx`$(\rho_B\mu^2_\ell, \mu(T) : T \in \mathcal{T}_0)$.
  - COMPUTE $\mathcal{T}_{\ell+1} := \mathcal{T}_\ell \oplus \mathcal{T}$.

Output: $\mathcal{T}_k$, η_k, μ_k, $\sigma_k := \sqrt{\eta^2_k + \mu^2_k}$ for $k = 0, 1, \ldots$.

The routine REFINE applies the newest vertex bisection [20] and refines the marked triangles $\mathcal{M}_\ell$ to compute the smallest admissible refinement $\mathcal{T}_{\ell+1}$ of $\mathcal{T}_\ell$ with $\mathcal{M}_\ell \subset \mathcal{T}_\ell \setminus \mathcal{T}_{\ell+1}$.

The data approximation algorithm `approx` used in Case B is introduced for separate marking in [8, Section 3.3] or [7, 17, 18] with input tolerance $\rho_B\mu^2_\ell$ and values $(\mu(T) : T \in \mathcal{T})$.

2.4 Axioms and Optimal Convergence

Suppose that there exist universal positive constants $\Lambda_1, \Lambda_2, \Lambda_3, \Lambda_4$ and $0 < \rho_2 < 1$ that satisfy (A1)–(A4) and (B1)–(B2) below. Here and in the following $\widehat{\mathcal{T}} \in \mathbb{T}(\mathcal{T})$ is an admissible triangulation and refinement of some $\mathcal{T} \in \mathbb{T} := \mathbb{T}(\mathcal{T}_0)$. Recall the definition of the error estimator in (2.2)–(2.4) and the abbreviation $\eta^2(\mathcal{T}, \mathcal{M}) := \sum_{M\in\mathcal{M}} \eta^2(\mathcal{T}, M)$ for all $\mathcal{M} \subseteq \mathcal{T}$.

(A1) *Stability:* For all $\mathcal{T} \in \mathbb{T}$ and all $\widehat{\mathcal{T}} \in \mathbb{T}(\mathcal{T})$,

$$|\eta(\widehat{\mathcal{T}}, \mathcal{T} \cap \widehat{\mathcal{T}}) - \eta(\mathcal{T}, \mathcal{T} \cap \widehat{\mathcal{T}})| \le \Lambda_1 \delta(\mathcal{T}, \widehat{\mathcal{T}}).$$

(A2) *Reduction:* For all $\mathcal{T} \in \mathbb{T}$ and all $\widehat{\mathcal{T}} \in \mathbb{T}(\mathcal{T})$,

$$\eta(\widehat{\mathcal{T}}, \widehat{\mathcal{T}} \setminus \mathcal{T}) \le \rho_2 \eta(\mathcal{T}, \mathcal{T} \setminus \widehat{\mathcal{T}}) + \Lambda_2 \delta(\mathcal{T}, \widehat{\mathcal{T}}).$$

(A3) *Discrete Reliability:* For all $\mathcal{T} \in \mathbb{T}$ and all $\widehat{\mathcal{T}} \in \mathbb{T}(\mathcal{T})$,

$$\delta^2(\mathcal{T}, \widehat{\mathcal{T}}) \le \Lambda_3(\eta^2(\mathcal{T}, \mathcal{T} \setminus \widehat{\mathcal{T}}) + \mu^2(\mathcal{T})).$$

Let $(\mathcal{T}_\ell)_{\ell\in\mathbb{N}}$ and $(\sigma_\ell)_{\ell\in\mathbb{N}}$ be the output of SAFEM of Section 2.3 and abbreviate $\eta_\ell := \eta(\mathcal{T}_\ell) \equiv \eta(\mathcal{T}_\ell, \mathcal{T}_\ell)$ and $\eta_\ell^2 := \eta^2(\mathcal{T}_\ell, \mathcal{T}_\ell) \equiv \eta^2(\mathcal{T}_\ell) := \eta(\mathcal{T}_\ell, \mathcal{T}_\ell)^2$, etc.

(A4) *Quasi-Orthogonality:* For all $\ell \in \mathbb{N}_0$,

$$\sum_{k=\ell}^{\infty} \delta^2(\mathcal{T}_k, \mathcal{T}_{k+1}) \le \Lambda_4 \sigma_\ell^2.$$

(B1) *Rate s Data Approximation:* There exists $s > 0$ such that for $\mathrm{Tol} > 0$, $\mathcal{T}_{\mathrm{Tol}} := \mathtt{approx}(\mathrm{Tol}, \mu(T) : T \in \mathcal{T}_0) \in \mathbb{T}$ satisfies

$$|\mathcal{T}_{\mathrm{Tol}}| - |\mathcal{T}_0| \le \Lambda_5 \mathrm{Tol}^{-\frac{1}{2s}} \quad \text{and} \quad \mu^2(\mathcal{T}_{\mathrm{Tol}}) \le \mathrm{Tol}.$$

(B2) *Quasimonotonicity of μ:* For all $\mathcal{T} \in \mathbb{T}(\mathcal{T})$ and all $\widehat{\mathcal{T}} \in \mathbb{T}(\mathcal{T})$,

$$\mu(\widehat{\mathcal{T}}) \le \mu(\mathcal{T}).$$

Theorem 2.1 (Quasi-Optimality [8]). *Suppose* (A1)–(A4) *and* (B1)–(B2). *Then there exists some $\kappa_0 > 0$ such that any choice of κ, θ_A and ρ_B with*

$$0 < \kappa < \kappa_1 := \min\{\kappa_0, \Lambda_1^{-2}\Lambda_3^{-1}\}, \quad 0 < \theta_A < \theta_0 := \frac{1 - \kappa\Lambda_1^2\Lambda_3}{1 + \Lambda_1^2\Lambda_3},$$

and $0 < \rho_B < 1$ implies the following. The output $(\mathcal{T}_\ell)_{\ell\in\mathbb{N}_0}$ and $(\sigma_\ell)_{\ell\in\mathbb{N}_0}$ of SAFEM (Algorithm 1) of Section 2.3 satisfies the equivalence

$$\Lambda_5^s + \sup_{\ell\in\mathbb{N}_0} (1 + |\mathcal{T}_\ell| - |\mathcal{T}_0|)^s \sigma_\ell \approx \Lambda_5^s + \sup_{N\in\mathbb{N}_0} (1 + N)^s \min \sigma(\mathbb{T}(N)).$$

The proof of Theorem 2.1 is given in [8] and not recalled here. The version of this paper is even slightly simplified in that $\widehat{\Lambda}_3 := 0$, $\Lambda_6 := 1$, and $\mathcal{R}(\mathcal{T}, \widehat{\mathcal{T}}) \equiv \mathcal{T} \setminus \widehat{\mathcal{T}}$ are more general in [8] and are not displayed explicitly in this paper.

The data approximation axioms (B1)–(B2) are discussed in [8], the results apply verbatim for the setting in this paper. This is exemplified in [8, Section 5] for the mixed FEM and hence not further detailed in this paper.

3 Verification of (A1)–(A2)

The analysis of (A1)–(A2) follows standard arguments and is outlined here for completeness for the problem at hand with piecewise constant coefficients with little emphasis that the global constants Λ_1, Λ_2 are bounded by the constant C_{jc} in the discrete jump control.

Lemma 3.1 (Discrete Jump Control [8]). *There exists a universal constant $C_{\rm jc}$, which depends on the interior angles in the regular triangulation $\mathcal{T}$ and the degree $k \in \mathbb{N}_0$, such that any $g \in P_k(\mathcal{T})$ with jumps*

$$[g]_E = \begin{cases} (g|_{T_+})|_E - (g|_{T_-})|_E & \text{for } E \in \mathcal{E}(\Omega) \text{ with } E = \partial T_+ \cap \partial T_-, \\ g|_E & \text{for } E \in \mathcal{E}(\partial\Omega) \cap \mathcal{E}(K) \end{cases}$$

satisfies

$$\sqrt{\sum_{K\in\mathcal{T}} |K|^{\frac{1}{2}} \sum_{E\in\mathcal{E}(K)} \|[g]_E\|^2_{L^2(E)}} \le C_{\rm jc}\|g\|_{L^2(\Omega)}.$$

The discrete jump control plus triangle inequalities in Lebesgue spaces and in finite-dimensional Euclidean spaces imply the stability (A1). Throughout this section, let $(\mathbf{p}_{\rm RT}, u_{\rm RT})$ and $(\widehat{\mathbf{p}_{\rm RT}}, \widehat{u_{\rm RT}})$ denote the discrete solution with respect to $\mathcal{T} \in \mathbb{T}$ and its refinement $\widehat{\mathcal{T}} \in \mathbb{T}(\mathcal{T})$, respectively, and let $\delta(\mathcal{T}, \widehat{\mathcal{T}})$ be the distance function (2.4).

Theorem 3.2 ((A1) Stability). *Axiom* (A1) *holds with $\Lambda_1^2 := 2(\underline{\varrho}^{-1} + \|\mathbf{b}^\star\|^2_\infty)(h^2_{\max} + C^2_{\rm jc})$ for a global lower bound $\underline{\varrho} > 0$ of the piecewise constant eigenvalues of the coefficient matrix $\mathbf{A}$, the supremum of $|\mathbf{b}^\star|$, the maximal mesh-size $h_{\max}$, and for the constant $C_{\rm jc}$ from the discrete jump control of Lemma 3.1.*

Proof. The reverse triangle inequality in $\mathbb{R}^m$ for $m := |\mathcal{T} \cap \widehat{\mathcal{T}}|$ over the element contributions implies that

$$|\eta(\widehat{\mathcal{T}}, \mathcal{T} \cap \widehat{\mathcal{T}}) - \eta(\mathcal{T}, \mathcal{T} \cap \widehat{\mathcal{T}})|^2 \le \sum_{T\in\mathcal{T}\cap\widehat{\mathcal{T}}} (\eta(\widehat{\mathcal{T}}, T) - \eta(\mathcal{T}, T))^2.$$

Each of the terms $\eta(\widehat{\mathcal{T}}, T)$ and $\eta(\mathcal{T}, T)$ is a norm in $\mathbb{R}^4$ of terms, which are Lebesgue norms and so allow for a reverse triangle inequality. This leads to

$$(\eta(\widehat{\mathcal{T}}, T) - \eta(\mathcal{T}, T))^2 \le |T|\|g\|^2_{L^2(T)} + |T|^{\frac{1}{2}} \sum_{E\in\mathcal{E}(T)} \|[g]\cdot\tau_E\|^2_{L^2(E)}$$

with the abbreviation $g := \mathbf{A}^{-1}(\widehat{\mathbf{p}_{\rm RT}} - \mathbf{p}_{\rm RT}) + (\widehat{u_{\rm RT}} - u_{\rm RT})\mathbf{b}^\star \in P_1(\widehat{\mathcal{T}}; \mathbb{R}^2)$. The sum over all $T \in \mathcal{T} \cap \widehat{\mathcal{T}}$ involves volume terms and edge jumps. Lemma 3.1 controls the latter terms and so results in

$$|\eta(\widehat{\mathcal{T}}, \mathcal{T} \cap \widehat{\mathcal{T}}) - \eta(\mathcal{T}, \mathcal{T} \cap \widehat{\mathcal{T}})|^2 \le C^2_{\rm jc}\|g\|^2_{L^2(\Omega)} + \sum_{T\in\mathcal{T}\cap\widehat{\mathcal{T}}} |T|\|g\|^2_{L^2(T)}.$$

The mesh-size is bounded from above and so the right-hand side is bounded by the factor $h^2_{\max} + C^2_{\rm jc}$ times the squared L^2 norm of g. A triangle inequality and the bounds on the coefficients show

$$\|g\|^2 \le 2(\underline{\varrho}^{-1} + \|\mathbf{b}^\star\|^2_\infty)\delta^2(\mathcal{T}, \widehat{\mathcal{T}}). \qquad \square$$

Theorem 3.3 ((A2) Reduction). *Axiom* (A2) *holds with $\varrho_2 := 2^{-\frac{1}{4}}$ and $\Lambda_2 := \Lambda_1$.*

Proof. For the m refined triangles $T \in \widehat{\mathcal{T}}(K) := \{T \in \widehat{\mathcal{T}} : T \subset K\}$ of $K \in \mathcal{T} \setminus \widehat{\mathcal{T}}$, the sum $\eta^2(\widehat{\mathcal{T}}, \widehat{\mathcal{T}} \setminus \mathcal{T})$ reads

$$\sum_{T\in\widehat{\mathcal{T}}\setminus\mathcal{T}} \Big(|T|\|\mathbf{A}^{-1}\widehat{\mathbf{p}_{\rm RT}} + \widehat{u_{\rm RT}}\mathbf{b}^\star\|^2_{L^2(T)} + |T|^{\frac{1}{2}} \sum_{F\in\mathcal{E}(T)} \|[\mathbf{A}^{-1}\widehat{\mathbf{p}_{\rm RT}} + \widehat{u_{\rm RT}}\mathbf{b}^\star]_F\cdot\tau_F\|^2_{L^2(F)} \Big).$$

The reverse triangle inequalities in $\mathbb{R}^{4m}$ and in Lebesgue spaces over triangles and edges and the abbreviation g from the previous proof plus $G := \mathbf{A}^{-1}\mathbf{p}_{\rm RT} + u_{\rm RT}\mathbf{b}^\star$ show

$$\eta(\widehat{\mathcal{T}}, \widehat{\mathcal{T}} \setminus \mathcal{T}) \le \Bigg(\sum_{\substack{K\in\mathcal{T}\setminus\widehat{\mathcal{T}} \\ T\in\widehat{\mathcal{T}}(K)}} \Big(|T|\|G\|^2_{L^2(T)} + |T|^{\frac{1}{2}} \sum_{E\in\mathcal{E}(T)} \|[G]_E\cdot\tau_E\|^2_{L^2(E)} \Big) \Bigg)^{\frac{1}{2}}$$
$$+ \Bigg(\sum_{T\in\widehat{\mathcal{T}}\setminus\mathcal{T}} \Big(|T|\|g\|^2_{L^2(T)} + |T|^{\frac{1}{2}} \sum_{E\in\mathcal{E}(T)} \|[g]_E\cdot\tau_E\|^2_{L^2(E)} \Big) \Bigg)^{\frac{1}{2}}.$$

Since $[G\cdot\tau_F]_F = 0$ for $F \in \widehat{\mathcal{E}}(\mathrm{int}(K))$ and $|T| \le \frac{|K|}{2}$ for $T \in \widehat{\mathcal{T}}(K)$, the first term on the right-hand side of the above displayed formula is bounded from above by $2^{-\frac{1}{4}}\eta(\mathcal{T}, \mathcal{T} \setminus \widehat{\mathcal{T}})$. The remaining term is estimated with Lemma 3.1 as in the previous proof and so with the same bound on $\Lambda_2 = \Lambda_1$. $\square$

4 Verification of (A3)

Throughout this section let $(\mathbf{p}_{\mathrm{RT}}, u_{\mathrm{RT}})$ and $(\widehat{\mathbf{p}_{\mathrm{RT}}}, \widehat{u_{\mathrm{RT}}})$ solve (1.4) and let $\Pi_0 f$ and $\widehat{\Pi}_0 f$ denote the L^2 orthogonal projection of the right-hand side f onto piecewise constants ($P_0(\mathcal{T})$ and $P_0(\widehat{\mathcal{T}})$) with respect to the triangulation $\mathcal{T}$ and its refinement $\widehat{\mathcal{T}}$, respectively.

The main residual R_1 is defined, for any test function $\widehat{\mathbf{q}_{\mathrm{RT}}} \in \mathrm{RT}_0(\widehat{\mathcal{T}})$, by

$$R_1(\widehat{\mathbf{q}_{\mathrm{RT}}}) := -(\mathbf{A}^{-1}\mathbf{p}_{\mathrm{RT}} + u_{\mathrm{RT}}\mathbf{b}^\star, \widehat{\mathbf{q}_{\mathrm{RT}}})_{L^2(\Omega)} + (\operatorname{div}\widehat{\mathbf{q}_{\mathrm{RT}}}, u_{\mathrm{RT}})_{L^2(\Omega)}. \tag{4.1}$$

Lemma 4.1. *There exists some* $\widehat{\mathbf{q}_{\mathrm{RT}}} \in \mathrm{RT}_0(\widehat{\mathcal{T}})$ *with norm* $\|\widehat{\mathbf{q}_{\mathrm{RT}}}\|_{H(\mathrm{div},\Omega)} = 1$ *and*

$$\delta(\mathcal{T}, \widehat{\mathcal{T}}) \lesssim R_1(\widehat{\mathbf{q}_{\mathrm{RT}}}) + \|\widehat{\Pi}_0 f - \Pi_0 f\|.$$

Proof. The initial mesh-size h_0 is sufficiently small throughout this paper to guarantee the existence and stability of the discrete solutions [4, Theorem 4.3]. The stability of the discrete problem (1.4) with respect to the refined triangulation $\widehat{\mathcal{T}}$ leads to the existence of $(\widehat{\mathbf{q}_{\mathrm{RT}}}, \widehat{v_{\mathrm{RT}}}) \in \mathrm{RT}_0(\widehat{\mathcal{T}}) \times P_0(\widehat{\mathcal{T}})$ with $\|\widehat{\mathbf{q}_{\mathrm{RT}}}\|_{H(\mathrm{div},\Omega)} + \|\widehat{v_{\mathrm{RT}}}\| \lesssim 1$ and

$$\begin{aligned}\delta(\mathcal{T}, \widehat{\mathcal{T}}) = (\mathbf{A}^{-1}(\widehat{\mathbf{p}_{\mathrm{RT}}} - \mathbf{p}_{\mathrm{RT}}) + (\widehat{u_{\mathrm{RT}}} - u_{\mathrm{RT}})\mathbf{b}^\star, \widehat{\mathbf{q}_{\mathrm{RT}}})_{L^2(\Omega)} - (\operatorname{div}\widehat{\mathbf{q}_{\mathrm{RT}}}, \widehat{u_{\mathrm{RT}}} - u_{\mathrm{RT}})_{L^2(\Omega)} \\ + (\operatorname{div}(\widehat{\mathbf{p}_{\mathrm{RT}}} - \mathbf{p}_{\mathrm{RT}}) + \gamma(\widehat{u_{\mathrm{RT}}} - u_{\mathrm{RT}}), \widehat{v_{\mathrm{RT}}})_{L^2(\Omega)}.\end{aligned}$$

Since $(\widehat{\mathbf{p}_{\mathrm{RT}}}, \widehat{u_{\mathrm{RT}}})$ solves (1.4) with respect to the refined triangulation $\widehat{\mathcal{T}}$ and $\operatorname{div}\mathbf{p}_{\mathrm{RT}} + \gamma u_{\mathrm{RT}} = \Pi_0 f$ (1.4) with respect to $\mathcal{T}$, this reads

$$\delta(\mathcal{T}, \widehat{\mathcal{T}}) = R_1(\widehat{\mathbf{q}_{\mathrm{RT}}}) + (\widehat{\Pi}_0 f - \Pi_0 f, \widehat{v_{\mathrm{RT}}})_{L^2(\Omega)}.$$

A Cauchy inequality concludes the proof. □

The further analysis of R_1 requires a discrete Helmholtz decomposition on a regular triangulation $\mathcal{T}$ of a (possibly) multi-connected domain Ω. The connectivity components $\Gamma_0, \Gamma_1, \ldots, \Gamma_J$ of $\partial\Omega$ are enumerated such that Γ_0 denotes the boundary of the unbounded component of $\mathbb{R}^2 \setminus \bar{\Omega}$. The modified lowest-order Crouzeix–Raviart space reads

$$\begin{aligned}\mathrm{CR}^1_\star(\mathcal{T}) = \{v \in \mathrm{CR}^1(\mathcal{T}) : \text{there exist } c_1, \ldots, c_J \in \mathbb{R}, c_0 := 0, \text{ such that for all } j = 0, 1, \ldots, J \\ \text{and all } E \in \mathcal{E}(\Gamma_j),\ v(\mathrm{mid}(E)) = c_j\}.\end{aligned} \tag{4.2}$$

(Here and throughout the paper, $\mathcal{E}(\Gamma_j)$ denotes the set of edges on Γ_j.)

Lemma 4.2 (Discrete Helmholtz Decomposition). *For the multi-connected domain* Ω *the decomposition of piecewise constant vector functions*

$$P_0(\mathcal{T}; \mathbb{R}^2) = \mathbf{A}\nabla_{\mathrm{NC}}\mathrm{CR}^1_\star(\mathcal{T}) \oplus \mathrm{Curl}(S^1(\mathcal{T}))$$

is orthogonal with respect to the L^2 *scalar product weighted by* $\mathbf{A}^{-1}$ *in the sense that*

$$(\nabla_{\mathrm{NC}} v_{\mathrm{CR}}, \mathrm{Curl}\, w_C)_{L^2(\Omega)} = 0 \quad \textit{for all } v_{\mathrm{CR}} \in \mathrm{CR}^1_\star(\mathcal{T}) \textit{ and all } w_C \in S^1(\mathcal{T}).$$

Proof. The discrete Helmholtz decomposition is well known for simply-connected domains and $J = 0$. The general case follows with the same argument by counting triangles and edges $|\mathcal{T}| + |\mathcal{N}| = |\mathcal{E}| + 1 - J$ in general; further details are omitted. □

The modified Crouzeix–Raviart space is accompanied by a modified Raviart–Thomas space $Q(\widehat{\mathcal{T}})$ with vanishing integral mean of the normal components over each boundary,

$$Q(\widehat{\mathcal{T}}) := \left\{\widehat{\mathbf{q}_{\mathrm{RT}}} \in \mathrm{RT}_0(\widehat{\mathcal{T}}) : \int_{\Gamma_j} \widehat{\mathbf{q}_{\mathrm{RT}}} \cdot \nu \,\mathrm{ds} = 0 \text{ for all } j = 1, \ldots, J\right\}.$$

The discrete Helmholtz decomposition allows for a characterization of the divergence-free functions.

Lemma 4.3 (Discrete Divergence). *The linear operator*

$$\operatorname{div} : Q(\widehat{\mathcal{T}}) \to P_0(\widehat{\mathcal{T}})$$

is surjective and its kernel is $\operatorname{Curl}(S^1(\widehat{\mathcal{T}}))$.

Proof. The divergence-free Raviart–Thomas functions in $Q(\widehat{\mathcal{T}})$ are piecewise constant and allow for a discrete Helmholtz decomposition as in Lemma 4.2. The decomposition implies that the divergence-free Raviart–Thomas functions in $Q(\widehat{\mathcal{T}})$ are those in $\operatorname{Curl}(S^1(\widehat{\mathcal{T}}))$. Consequently, the kernel of $\operatorname{div} : Q(\widehat{\mathcal{T}}) \to P_0(\widehat{\mathcal{T}})$ has the dimension $|\widehat{\mathcal{N}}| - 1$ for the number $|\widehat{\mathcal{N}}|$ of nodes in $\widehat{\mathcal{T}}$. Since the dimension of the vector space $Q(\widehat{\mathcal{T}})$ is $|\widehat{\mathcal{E}}| - J$ for the number $|\widehat{\mathcal{E}}|$ of edges in $\widehat{\mathcal{T}}$, the range of $\operatorname{div} : Q(\widehat{\mathcal{T}}) \to P_0(\widehat{\mathcal{T}})$ has dimension $|\widehat{\mathcal{E}}| - |\widehat{\mathcal{N}}| + 1 - J$. Since $|\widehat{\mathcal{T}}| + |\widehat{\mathcal{N}}| = |\widehat{\mathcal{E}}| + 1 - J$, the range is $P_0(\widehat{\mathcal{T}})$. □

One key argument of the reliability analysis is the split of the difference $\widehat{\mathbf{p}_{\mathrm{RT}}} - \mathbf{p}_{\mathrm{RT}}$ into two parts $\widehat{\mathbf{p}_{\mathrm{RT}}} - \widehat{\mathbf{p}_{\mathrm{RT}}}^\star$ and $\widehat{\mathbf{p}_{\mathrm{RT}}}^\star - p_{\mathrm{RT}}$ for some auxiliary solution: Seek $(\widehat{\mathbf{p}_{\mathrm{RT}}}^\star, \widehat{u_{\mathrm{RT}}}^\star) \in \mathrm{RT}_0(\widehat{\mathcal{T}}) \times P_0(\widehat{\mathcal{T}})$ with

$$\int_{\Gamma_j} \widehat{\mathbf{p}_{\mathrm{RT}}}^\star \cdot \nu \, \mathrm{ds} = \int_{\Gamma_j} \mathbf{p}_{\mathrm{RT}} \cdot \nu \, \mathrm{ds}, \tag{4.3a}$$

$$(\mathbf{A}^{-1}\widehat{\mathbf{p}_{\mathrm{RT}}}^\star, \widehat{\mathbf{q}_{\mathrm{RT}}})_{L^2(\Omega)} - (\operatorname{div} \widehat{\mathbf{q}_{\mathrm{RT}}}, \widehat{u_{\mathrm{RT}}}^\star)_{L^2(\Omega)} = -(u_{\mathrm{RT}}\mathbf{b}^\star, \widehat{\mathbf{q}_{\mathrm{RT}}})_{L^2(\Omega)}, \tag{4.3b}$$

$$(\operatorname{div} \widehat{\mathbf{p}_{\mathrm{RT}}}^\star, \widehat{v_{\mathrm{RT}}})_{L^2(\Omega)} = (\Pi_0 f - \gamma u_{\mathrm{RT}}, \widehat{v_{\mathrm{RT}}})_{L^2(\Omega)} \tag{4.3c}$$

hold for all $\widehat{\mathbf{q}_{\mathrm{RT}}} \in Q(\widehat{\mathcal{T}})$, for all $\widehat{v_{\mathrm{RT}}} \in P_0(\widehat{\mathcal{T}})$, and for all $j = 1, \dots, J$.

The solution to (4.3) is recovered from an auxiliary nonconforming problem: Let $\widehat{u_{\mathrm{CR}}}^\star \in \mathrm{CR}^1_\star(\widehat{\mathcal{T}})$ denote the Riesz representation of the functional on the right-hand side of

$$\begin{aligned}(\mathbf{A}\nabla_{\mathrm{NC}}\widehat{u_{\mathrm{CR}}}^\star, \nabla_{\mathrm{NC}}\widehat{w_{\mathrm{CR}}})_{L^2(\Omega)} &= (\Pi_0 f - \gamma u_{\mathrm{RT}}, \widehat{w_{\mathrm{CR}}})_{L^2(\Omega)} - (u_{\mathrm{RT}}\mathbf{b}, \nabla_{\mathrm{NC}}\widehat{w_{\mathrm{CR}}})_{L^2(\Omega)} \\ &\quad - \sum_{j=1}^{J} \left(\fint_{\Gamma_j} \mathbf{p}_{\mathrm{RT}} \cdot \nu \, \mathrm{ds} \right) \left(\int_{\Gamma_j} \widehat{w_{\mathrm{CR}}} \, \mathrm{ds} \right)\end{aligned} \tag{4.4}$$

for all test functions $\widehat{w_{\mathrm{CR}}} \in \mathrm{CR}^1_\star(\widehat{\mathcal{T}})$ in the Hilbert space $(\mathrm{CR}^1_\star(\widehat{\mathcal{T}}), (\mathbf{A}\nabla_{\mathrm{NC}}\bullet, \nabla_{\mathrm{NC}}\bullet)_{L^2(\Omega)})$. Here and throughout the paper, $\fint$ denotes the integral mean $\fint_{\Gamma_j} \bullet \, ds := \int_{\Gamma_j} \bullet \, ds / |\Gamma_j|$ for the length $|\Gamma_j|$ of the closed polygon Γ_j.

The equivalence of this with (4.3) implies the unique solvability of (4.3). To verify this, let $\widehat{u_{\mathrm{CR}}}^\star$ solve (4.4) and, for $\mathbf{x} \in T \in \widehat{\mathcal{T}}$, set

$$S(T) := \fint_T (\mathbf{x} - \operatorname{mid}(T)) \cdot \mathbf{A}^{-1}(\mathbf{x} - \operatorname{mid}(T)) \, \mathrm{dx},$$

$$\widehat{\mathbf{p}_{\mathrm{RT}}}^\star(\mathbf{x}) := -(\mathbf{A}\nabla_{\mathrm{NC}}\widehat{u_{\mathrm{CR}}}^\star + u_{\mathrm{RT}}\mathbf{b}) + \frac{1}{2}(\Pi_0 f - \gamma u_{\mathrm{RT}})(\mathbf{x} - \operatorname{mid}(T)), \tag{4.5}$$

$$\widehat{u_{\mathrm{RT}}}^\star(\mathbf{x}) := \Pi_0 \widehat{u_{\mathrm{CR}}}^\star + S(T)(\Pi_0 f - \gamma u_{\mathrm{RT}}). \tag{4.6}$$

The piecewise constant function $S(\mathcal{T})$ is

$$S(\mathcal{T})|_T = S(T) := \frac{1}{4} \fint_T (\mathbf{x} - \operatorname{mid}(T)) \cdot \mathbf{A}^{-1}((\mathbf{x} - \operatorname{mid}(T)) \, \mathrm{dx}$$

in $T \in \mathcal{T}$.

Lemma 4.4. *The pair* $(\widehat{\mathbf{p}_{\mathrm{RT}}}^\star, \widehat{u_{\mathrm{RT}}}^\star)$ *from* (4.5)–(4.6) *defines the unique solution to* (4.3).

Proof. The proof imitates that of [4, Theorem 4.2] and generalizes it to multiply connected domains. The arguments therein confirm the continuity of normal components along the interior edges and prove $\widehat{\mathbf{p}_{\mathrm{RT}}}^\star \in \mathrm{RT}_0(\widehat{\mathcal{T}}) \subset H(\operatorname{div}, \Omega)$. The present situation involves the connectivity components $\Gamma_1, \dots, \Gamma_J$ of the boundary $\partial\Omega$ and requires a little modification in the proof that $(\widehat{\mathbf{p}_{\mathrm{RT}}}^\star, \widehat{u_{\mathrm{RT}}}^\star)$ indeed satisfies (4.3). Set

$$c_j := \fint_{\Gamma_j} \widehat{u_{\mathrm{CR}}}^\star \, \mathrm{ds}$$

and substitute $\widehat{\mathbf{p}_{\mathrm{RT}}}^\star$ from (4.5) before a piecewise integration by parts shows, for any test function $\widehat{\mathbf{q}_{\mathrm{RT}}} \in Q(\widehat{\mathcal{T}})$, that

$$\begin{aligned}&(\widehat{\mathbf{p}_{\mathrm{RT}}}^\star + u_{\mathrm{RT}}\mathbf{b}^\star, \widehat{\mathbf{q}_{\mathrm{RT}}})_{L^2(\Omega)} - (\operatorname{div}\widehat{\mathbf{q}_{\mathrm{RT}}}, \Pi_0\widehat{u_{\mathrm{CR}}}^\star)_{L^2(\Omega)}\\ &\quad= \Big(\frac{1}{2}\mathbf{A}^{-1}(\Pi_0 f - \gamma u_{\mathrm{RT}})(\bullet - \operatorname{mid}(\mathcal{T})), \widehat{\mathbf{q}_{\mathrm{RT}}}\Big)_{L^2(\Omega)} - \sum_{j=1}^{J} c_j \int_{\Gamma_j} (\widehat{\mathbf{q}_{\mathrm{RT}}}\cdot\nu)\,\mathrm{ds}.\end{aligned}$$

The first term on the right-hand side already appears in [4, p. 567, lines 1–2] and is rewritten as

$$2((\Pi_0 f - \gamma u_{\mathrm{RT}})\mathbf{A}^{-1}(\bullet - \operatorname{mid}(\mathcal{T})), \widehat{\mathbf{q}_{\mathrm{RT}}})_{L^2(\Omega)} = (\Pi_0 f - \gamma u_{\mathrm{RT}}, S(\mathcal{T})\operatorname{div}\widehat{\mathbf{q}_{\mathrm{RT}}})_{L^2(\Omega)}.$$

This term combines with $-(\operatorname{div}\widehat{\mathbf{q}_{\mathrm{RT}}}, \Pi_0\widehat{u_{\mathrm{CR}}}^\star)_{L^2(\Omega)}$ in the aforementioned equality and leads with (4.6) to $-(\operatorname{div}\widehat{\mathbf{q}_{\mathrm{RT}}}, \widehat{u_{\mathrm{RT}}}^\star)_{L^2(\Omega)}$. Recall that $c_0 = 0$ and that $\int_{\Gamma_j}\widehat{\mathbf{q}_{\mathrm{RT}}}\cdot\nu\,\mathrm{ds} = 0$ for $j = 1, \dots, J$ because of $\widehat{\mathbf{q}_{\mathrm{RT}}} \in Q(\widehat{\mathcal{T}})$. This calculation leads to equation (4.3b). Since $\widehat{\mathbf{p}_{\mathrm{RT}}}^\star \in \mathrm{RT}_0(\widehat{\mathcal{T}}) \subset H(\operatorname{div}, \Omega)$, the definition of (4.5) immediately proves (4.3c). Rewrite (4.5) to obtain an identity for $\mathbf{A}\nabla_{\mathrm{NC}}\widehat{u_{\mathrm{CR}}}^\star$ and utilize this in (4.4). This leads to an identity, which allows a piecewise integration by parts and then results in

$$\sum_{j=1}^{J}\int_{\Gamma_j}\widehat{w_{\mathrm{CR}}}(\widehat{\mathbf{p}_{\mathrm{RT}}}^\star - \mathbf{p}_{\mathrm{RT}})\cdot\nu\,\mathrm{ds} = 0 \quad \text{for all } \widehat{w_{\mathrm{CR}}} \in \mathrm{CR}^1_\star(\widehat{\mathcal{T}}).$$

The design of $\widehat{w_{\mathrm{CR}}} \in \mathrm{CR}^1_\star(\widehat{\mathcal{T}})$ with piecewise integral means along the boundary edges of Γ_j which are constant for each $j = 1, \dots, J$ proves (4.3a).

This concludes the proof of the existence of a discrete solution to (4.3a)–(4.3c) and it remains to show the uniqueness of a discrete solution. This follows from the trivial solution to the homogeneous system

$$(\mathbf{A}^{-1}\widehat{\mathbf{p}_{\mathrm{RT}}}^\star, \widehat{\mathbf{q}_{\mathrm{RT}}})_{L^2(\Omega)} - (\operatorname{div}\widehat{\mathbf{q}_{\mathrm{RT}}}, \widehat{u_{\mathrm{RT}}}^\star)_{L^2(\Omega)} = 0 = (\operatorname{div}\widehat{\mathbf{p}_{\mathrm{RT}}}^\star, \widehat{v_{\mathrm{RT}}})_{L^2(\Omega)}$$

for all $\widehat{\mathbf{q}_{\mathrm{RT}}} \in Q(\widehat{\mathcal{T}})$, $\widehat{v_{\mathrm{RT}}} \in P_0(\widehat{\mathcal{T}})$ plus $\int_{\Gamma_j}\widehat{\mathbf{p}_{\mathrm{RT}}}^\star\cdot\nu\,\mathrm{ds} = 0$ for $j = 0, \dots, J$. Given an arbitrary solution $(\widehat{\mathbf{p}_{\mathrm{RT}}}^\star, \widehat{u_{\mathrm{RT}}}^\star)$ to this discrete homogeneous problem, let $\widehat{\mathbf{q}_{\mathrm{RT}}} = \widehat{\mathbf{p}_{\mathrm{RT}}}^\star$ to find $\widehat{\mathbf{p}_{\mathrm{RT}}}^\star = 0$. It follows $(\operatorname{div}\widehat{\mathbf{q}_{\mathrm{RT}}}, \widehat{u_{\mathrm{RT}}}^\star)_{L^2(\Omega)} = 0$ for all test functions. Lemma 4.3 allows for a test function $\widehat{\mathbf{q}_{\mathrm{RT}}}$ with $\operatorname{div}\widehat{\mathbf{q}_{\mathrm{RT}}} = \widehat{u_{\mathrm{RT}}}^\star$ and so $\widehat{u_{\mathrm{RT}}}^\star = 0$. This concludes the proof of the uniqueness of the solution of the homogeneous system. □

Lemma 4.5. *The test function $\widehat{\mathbf{q}_{\mathrm{RT}}} \in \mathrm{RT}_0(\widehat{\mathcal{T}})$ in Lemma 4.1 can be selected additionally to satisfy $\Pi_0\operatorname{div}\widehat{\mathbf{q}_{\mathrm{RT}}} = 0$ and $\int_{\Gamma_j}\widehat{\mathbf{q}_{\mathrm{RT}}}\cdot\nu\,\mathrm{ds} = 0$ for all $j = 0, 1, \dots, J$.*

Proof. The first equation in (1.4) shows that $\mathrm{RT}_0(\mathcal{T})$ belongs to the kernel of R_1 from (4.1). Hence we may and will replace test function $\widehat{\mathbf{q}_{\mathrm{RT}}} \in \mathrm{RT}_0(\widehat{\mathcal{T}})$ in Lemma 4.1 by $\widehat{\mathbf{q}_{\mathrm{RT}}} - \mathbf{q}_{\mathrm{RT}}$ for some appropriate $\mathbf{q}_{\mathrm{RT}} \in \mathrm{RT}_0(\mathcal{T})$. The naive choice of the Fortin interpolation $\mathbf{q}_{\mathrm{RT}}$ of $\widehat{\mathbf{q}_{\mathrm{RT}}}$ leads to the additional properties but leaves open the subtle question of the uniform bound $\|\mathbf{q}_{\mathrm{RT}}\|_{H(\operatorname{div},\Omega)}$ in terms of $\|\widehat{\mathbf{q}_{\mathrm{RT}}}\|_{H(\operatorname{div},\Omega)} \approx 1$. This proof utilizes the MFEM solution $(\mathbf{q}_{\mathrm{RT}}, v_{\mathrm{RT}}) \in \mathrm{RT}_0(\mathcal{T})\times P_0(\mathcal{T})$ to the modified Poisson model problem with right-hand side $\Pi_0\operatorname{div}\widehat{\mathbf{q}_{\mathrm{RT}}}$,

$$\int_{\Gamma_j}\mathbf{q}_{\mathrm{RT}}\cdot\nu\,\mathrm{ds} = \int_{\Gamma_j}\widehat{\mathbf{q}_{\mathrm{RT}}}\cdot\nu\,\mathrm{ds} \qquad \text{for all } j = 1, \dots, J, \tag{4.7a}$$

$$(\mathbf{q}_{\mathrm{RT}}, \mathbf{z}_{\mathrm{RT}})_{L^2(\Omega)} = (\operatorname{div}\mathbf{z}_{\mathrm{RT}}, v_{\mathrm{RT}})_{L^2(\Omega)} \qquad \text{for all } \mathbf{z}_{\mathrm{RT}} \in \mathrm{RT}_0(\mathcal{T}), \tag{4.7b}$$

$$(\operatorname{div}\mathbf{q}_{\mathrm{RT}}, w_{\mathrm{RT}})_{L^2(\Omega)} = (\Pi_0\operatorname{div}\widehat{\mathbf{q}_{\mathrm{RT}}}, w_{\mathrm{RT}})_{L^2(\Omega)} \qquad \text{for all } w_{\mathrm{RT}} \in P_0(\mathcal{T}). \tag{4.7c}$$

Equations (4.7) are a particular version of (4.3) and the equivalence of Lemma 4.4 applies here as well. This implies the unique existence of $(\mathbf{q}_{\mathrm{RT}}, v_{\mathrm{RT}}) \in \mathrm{RT}(\mathcal{T}) \times P_0(\mathcal{T})$ and leads the desired bound

$$\|\mathbf{q}_{\mathrm{RT}}\|_{H(\operatorname{div},\Omega)} \lesssim \|\widehat{\mathbf{q}_{\mathrm{RT}}}\|_{H(\operatorname{div},\Omega)} \approx 1.$$

□

Recall that $(\mathbf{p}_{\mathrm{RT}}, u_{\mathrm{RT}})$ and $(\widehat{\mathbf{p}_{\mathrm{RT}}}, \widehat{u_{\mathrm{RT}}})$ solve (1.4) with respect to the triangulation $\mathcal{T}$ and its refinement $\widehat{\mathcal{T}}$, respectively, and that $(\widehat{\mathbf{p}_{\mathrm{RT}}}^\star, \widehat{u_{\mathrm{RT}}}^\star)$ solves (4.3). Define the modified residual R_2 by

$$R_2(\widehat{\mathbf{q}_{\mathrm{RT}}}) := -(\mathbf{A}^{-1}\widehat{\mathbf{p}_{\mathrm{RT}}}^\star + u_{\mathrm{RT}}\mathbf{b}^\star, \widehat{\mathbf{q}_{\mathrm{RT}}})_{L^2(\Omega)} \quad \text{for any test function } \widehat{\mathbf{q}_{\mathrm{RT}}} \in \mathrm{RT}_0(\widehat{\mathcal{T}}). \tag{4.8}$$

Lemma 4.5 and the modified test-function $\widehat{\mathbf{q}_{\mathrm{RT}}}$ show

$$\begin{aligned}\delta(\mathcal{T},\widehat{\mathcal{T}})-\|\widehat{\Pi}_0 f-\Pi_0 f\| &\le R_1(\widehat{\mathbf{q}_{\mathrm{RT}}})=-(\mathbf{A}^{-1}\mathbf{p}_{\mathrm{RT}}+u_{\mathrm{RT}}\mathbf{b}^\star,\widehat{\mathbf{q}_{\mathrm{RT}}})_{L^2(\Omega)}\\ &\lesssim R_2(\widehat{\mathbf{q}_{\mathrm{RT}}})+\|\widehat{\mathbf{p}_{\mathrm{RT}}}^\star-\mathbf{p}_{\mathrm{RT}}\|_{H(\mathrm{div},\Omega)}.\end{aligned}\tag{4.9}$$

The divergence-free term $\widehat{\mathbf{p}_{\mathrm{RT}}}^\star-\mathbf{p}_{\mathrm{RT}}$ is controlled in the subsequent lemma.

Lemma 4.6. *It holds* $\|\widehat{\mathbf{p}_{\mathrm{RT}}}^\star-\mathbf{p}_{\mathrm{RT}}\|_{H(\mathrm{div},\Omega)}\lesssim\eta(\mathcal{T},\mathcal{T}\setminus\widehat{\mathcal{T}})$.

Proof. Since $\operatorname{div}\widehat{\mathbf{p}_{\mathrm{RT}}}^\star=\Pi_0 f-\gamma u_{\mathrm{RT}}=\operatorname{div}\mathbf{p}_{\mathrm{RT}}$ implies $\operatorname{div}(\widehat{\mathbf{p}_{\mathrm{RT}}}^\star-\mathbf{p}_{\mathrm{RT}})=0$, it follows that $\widehat{\mathbf{p}_{\mathrm{RT}}}^\star-\mathbf{p}_{\mathrm{RT}}$ is piecewise constant and its discrete Helmholtz decomposition leads to $\widehat{\alpha_{\mathrm{CR}}}\in\mathrm{CR}^1_\star(\widehat{\mathcal{T}})$ and $\widehat{\beta_C}\in S^1(\widehat{\mathcal{T}})$ with

$$\widehat{\mathbf{p}_{\mathrm{RT}}}^\star-\mathbf{p}_{\mathrm{RT}}=\mathbf{A}\nabla_{\mathrm{NC}}\widehat{\alpha_{\mathrm{CR}}}+\operatorname{Curl}\widehat{\beta_C}.$$

This and the L^2 orthogonality $(\widehat{\mathbf{p}_{\mathrm{RT}}}^\star-\mathbf{p}_{\mathrm{RT}})\perp\nabla_{\mathrm{NC}}\widehat{\alpha_{\mathrm{CR}}}$ show that $\widehat{\alpha_{\mathrm{CR}}}\equiv 0$. Consequently,

$$\|\widehat{\mathbf{p}_{\mathrm{RT}}}^\star-\mathbf{p}_{\mathrm{RT}}\|^2_{H(\mathrm{div},\Omega)}=(\widehat{\mathbf{p}_{\mathrm{RT}}}^\star-\mathbf{p}_{\mathrm{RT}},\mathbf{A}^{-1}\operatorname{Curl}\widehat{\beta_C})_{L^2(\Omega)}.\tag{4.10}$$

Given any node $z\in\mathcal{N}$ in the coarse triangulation $\mathcal{T}$, the Scott–Zhang quasi-interpolation [19] defines $\beta_C(z)$ by a selection of an edge $E(z)\in\mathcal{E}$ with vertex z and evaluates some weighted integral of $\widehat{\beta_C}$ along $E(z)$. Select the edge $E(z)\in\mathcal{E}\cap\widehat{\mathcal{E}}$ if possible to obtain a Scott–Zhang quasi-interpolation $\beta_C\in S^1(\mathcal{T})$ of $\widehat{\beta_C}$ with $\widehat{\beta_C}-\beta_C=0$ a.e. in $\bigcup(\mathcal{T}\cap\widehat{\mathcal{T}})$ plus the local approximation and stability properties. For any edge $E\in\mathcal{E}$ of length h_E and its neighborhood $\Omega(E):=\bigcup_{z\in\mathcal{N}(E)}\omega_z$ for the nodal patches ω_z, the latter properties and discrete trace inequalities result in

$$\|\widehat{\beta_C}-\beta_C\|_{L^2(E)}\lesssim h_E^{\frac12}\|\widehat{\beta_C}\|_{H^1(\Omega(E))}.\tag{4.11}$$

The weak formulation (1.4) with $\mathbf{q}_{\mathrm{RT}}=\operatorname{Curl}\beta_C\in\mathrm{RT}_0(\mathcal{T})$ and equation (4.3b) with $\widehat{\mathbf{q}_{\mathrm{RT}}}:=\operatorname{Curl}\beta_C\in\mathrm{RT}_0(\widehat{\mathcal{T}})$ show $(\widehat{\mathbf{p}_{\mathrm{RT}}}^\star-\mathbf{p}_{\mathrm{RT}},\mathbf{A}^{-1}\operatorname{Curl}\beta_C)_{L^2(\Omega)}=0$. Hence (4.10) is $(\widehat{\mathbf{p}_{\mathrm{RT}}}^\star-\mathbf{p}_{\mathrm{RT}},\mathbf{A}^{-1}\operatorname{Curl}(\widehat{\beta_C}-\beta_C))_{L^2(\Omega)}$. The test function $\widehat{\mathbf{q}_{\mathrm{RT}}}:=\operatorname{Curl}(\widehat{\beta_C}-\beta_C)$ in equation (4.3b) shows that (4.10) is $(\mathbf{A}^{-1}\mathbf{p}_{\mathrm{RT}}+u_{\mathrm{RT}}\mathbf{b}^\star,\operatorname{Curl}(\beta_C-\widehat{\beta_C}))_{L^2(\Omega)}$. This and a piecewise integration by parts leads to

$$\|\widehat{\mathbf{p}_{\mathrm{RT}}}^\star-\mathbf{p}_{\mathrm{RT}}\|^2_{H(\mathrm{div},\Omega)}=\sum_{E\in\widehat{\mathcal{E}}}\int_E(\beta_C-\widehat{\beta_C})[\mathbf{A}^{-1}\mathbf{p}_{\mathrm{RT}}+u_{\mathrm{RT}}\mathbf{b}^\star]_E\cdot\tau_E\,\mathrm{d}s-\sum_{T\in\widehat{\mathcal{T}}}\int_T(\beta_C-\widehat{\beta_C})\operatorname{curl}(\mathbf{A}^{-1}\mathbf{p}_{\mathrm{RT}}+u_{\mathrm{RT}}\mathbf{b}^\star)\,\mathrm{d}s.$$

The piecewise curl of the low-order Raviart–Thomas finite element functions vanishes and so do all summands in the last term. Since $\widehat{\beta_C}-\beta_C=0$ along any edge $E\in\mathcal{E}\cap\widehat{\mathcal{E}}$, this proves

$$\|\widehat{\mathbf{p}_{\mathrm{RT}}}^\star-\mathbf{p}_{\mathrm{RT}}\|^2_{H(\mathrm{div},\Omega)}\lesssim\sum_{E\in\mathcal{E}\setminus\widehat{\mathcal{E}}}\|[\mathbf{A}^{-1}\mathbf{p}_{\mathrm{RT}}+u_{\mathrm{RT}}\mathbf{b}^\star]_E\cdot\tau_E\|_{L^2(E)}\|\widehat{\beta_C}-\beta_C\|_{L^2(E)}.$$

The combination with estimate (4.11) for $\|\widehat{\beta_C}-\beta_C\|_{L^2(E)}$ and the bound $\|\nabla\widehat{\beta_C}\|=\|\operatorname{Curl}\widehat{\beta_C}\|\lesssim\|\widehat{\mathbf{p}_{\mathrm{RT}}}^\star-\mathbf{p}_{\mathrm{RT}}\|_{H(\mathrm{div},\Omega)}$ imply

$$\|\widehat{\mathbf{p}_{\mathrm{RT}}}^\star-\mathbf{p}_{\mathrm{RT}}\|^2_{H(\mathrm{div},\Omega)}\lesssim\sum_{E\in\mathcal{E}\setminus\widehat{\mathcal{E}}}h_E\|[\mathbf{A}^{-1}\mathbf{p}_{\mathrm{RT}}+u_{\mathrm{RT}}\mathbf{b}^\star]_E\cdot\tau_E\|^2_{L^2(E)}.\tag{4.12}$$

A rearrangement with the triangle-oriented error estimator concludes the proof. □

Lemma 4.7. *The test function* $\widehat{\mathbf{q}_{\mathrm{RT}}}$ *from Lemma 4.5 and the residual* R_2 *from* (4.8) *satisfy*

$$R_2(\widehat{\mathbf{q}_{\mathrm{RT}}})\lesssim\eta(\mathcal{T},\mathcal{T}\setminus\widehat{\mathcal{T}})+\|\widehat{\mathbf{p}_{\mathrm{RT}}}^\star-\mathbf{p}_{\mathrm{RT}}\|_{H(\mathrm{div},\Omega)}.$$

Proof. Let $\bullet-\operatorname{mid}(\widehat{\mathcal{T}})\in P_1(\widehat{\mathcal{T}};\mathbb{R}^2)$ abbreviate the function $x-\operatorname{mid}(T)$ for $x\in T\in\widehat{\mathcal{T}}$ and consider the test function $\widehat{\mathbf{q}_{\mathrm{RT}}}=\widehat{\Pi}_0\widehat{\mathbf{q}_{\mathrm{RT}}}+\frac12\operatorname{div}\widehat{\mathbf{q}_{\mathrm{RT}}}(\bullet-\operatorname{mid}(\widehat{\mathcal{T}}))\in P_1(\widehat{\mathcal{T}};\mathbb{R}^2)$ from Lemma 4.5. The piecewise constant part $\widehat{\Pi}_0\widehat{\mathbf{q}_{\mathrm{RT}}}$ allows a discrete Helmholtz decomposition

$$\widehat{\Pi}_0\widehat{\mathbf{q}_{\mathrm{RT}}}=\mathbf{A}\nabla_{\mathrm{NC}}\widehat{v_{\mathrm{CR}}}+\operatorname{Curl}\widehat{\beta_C}$$

from Lemma 4.2 for some $\widehat{v_{\mathrm{CR}}}\in\mathrm{CR}^1_\star(\widehat{\mathcal{T}})$ and some $\widehat{\beta_C}\in S^1(\widehat{\mathcal{T}})$. Altogether, there are three contributions of

$$R_2(\widehat{\mathbf{q}_{\mathrm{RT}}})=R_2(\mathbf{A}\nabla_{\mathrm{NC}}\widehat{v_{\mathrm{CR}}})+R_2(\operatorname{Curl}\widehat{\beta_C})+R_2\Big(\frac12\operatorname{div}\widehat{\mathbf{q}_{\mathrm{RT}}}(\bullet-\operatorname{mid}(\widehat{\mathcal{T}}))\Big).$$

(i) The representation of $\widehat{\mathbf{p}_{\mathrm{RT}}}^\star$ in (4.5) is utilized in the first contribution and leads to

$$R_2(\mathbf{A}\nabla_{\mathrm{NC}}\widehat{v_{\mathrm{CR}}}) = -(\widehat{\mathbf{p}_{\mathrm{RT}}}^\star + u_{\mathrm{RT}}\mathbf{b}, \nabla_{\mathrm{NC}}\widehat{v_{\mathrm{CR}}})_{L^2(\Omega)} = (\nabla_{\mathrm{NC}}\widehat{u_{\mathrm{CR}}}^\star, \mathbf{A}\nabla_{\mathrm{NC}}\widehat{v_{\mathrm{CR}}})_{L^2(\Omega)}.$$

On the other hand, $\mathbf{A}\nabla_{\mathrm{NC}}\widehat{v_{\mathrm{CR}}} = \widehat{\Pi}_0\widehat{\mathbf{q}_{\mathrm{RT}}} - \operatorname{Curl}\widehat{\beta_C}$ is L^2 orthogonal to $\nabla_{\mathrm{NC}}\widehat{u_{\mathrm{CR}}}^\star$. This and an integration by parts prove

$$R_2(\mathbf{A}\nabla_{\mathrm{NC}}\widehat{v_{\mathrm{CR}}}) = (\nabla_{\mathrm{NC}}\widehat{u_{\mathrm{CR}}}^\star, \widehat{\mathbf{q}_{\mathrm{RT}}})_{L^2(\Omega)} = -(\widehat{u_{\mathrm{CR}}}^\star, \operatorname{div}\widehat{\mathbf{q}_{\mathrm{RT}}})_{L^2(\Omega)}.$$

Recall that $\operatorname{div}\widehat{\mathbf{q}_{\mathrm{RT}}}$ is L^2 orthogonal onto $P_0(\mathcal{T})$ and so

$$R_2(\mathbf{A}\nabla_{\mathrm{NC}}\widehat{v_{\mathrm{CR}}}) = ((\Pi_0 - \widehat{\Pi}_0)\widehat{u_{\mathrm{CR}}}^\star, \operatorname{div}\widehat{\mathbf{q}_{\mathrm{RT}}})_{L^2(\Omega)} \le \|(\widehat{\Pi}_0 - \Pi_0)\widehat{u_{\mathrm{CR}}}^\star\|\,\|\operatorname{div}\widehat{\mathbf{q}_{\mathrm{RT}}}\|.$$

Note that $(\widehat{\Pi}_0 - \Pi_0)\widehat{u_{\mathrm{CR}}}^\star$ vanishes a.e. in $T \in \mathcal{T}\cap\widehat{\mathcal{T}}$ and a piecewise discrete Poincaré inequality shows $\|(\widehat{\Pi}_0 - \Pi_0)\widehat{u_{\mathrm{CR}}}^\star\| \lesssim \|h_{\mathcal{T}}\nabla_{\mathrm{NC}}\widehat{u_{\mathrm{CR}}}^\star\|_{L^2(\Omega')}$ with the interior Ω' of the domain $\bigcup(\mathcal{T}\setminus\widehat{\mathcal{T}})$. Consequently,

$$R_2(\mathbf{A}\nabla_{\mathrm{NC}}\widehat{v_{\mathrm{CR}}}) \lesssim \|h_{\mathcal{T}}\nabla_{\mathrm{NC}}\widehat{u_{\mathrm{CR}}}^\star\|_{L^2(\Omega')}.$$

(ii) Observe from (4.3b) and $\operatorname{Curl}\widehat{\beta_C} \in Q(\widehat{\mathcal{T}})$ that $R_2(\operatorname{Curl}\widehat{\beta_C}) = 0$.

(iii) Since $\operatorname{div}\widehat{\mathbf{q}_{\mathrm{RT}}}$ vanishes outside the set Ω' (for $\operatorname{div}\widehat{\mathbf{q}_{\mathrm{RT}}} = \Pi_0\operatorname{div}\widehat{\mathbf{q}_{\mathrm{RT}}}$ on $T \in \mathcal{T}\cap\widehat{\mathcal{T}}$) and the weight satisfies $|\bullet - \operatorname{mid}(\widehat{\mathcal{T}})| \lesssim h_{\mathcal{T}}$, the term $R_2(\frac{1}{2}\operatorname{div}\widehat{\mathbf{q}_{\mathrm{RT}}}(\bullet - \operatorname{mid}(\widehat{\mathcal{T}})))$ is equal to

$$-\frac{1}{2}(\mathbf{A}^{-1}\widehat{\mathbf{p}_{\mathrm{RT}}}^\star + u_{\mathrm{RT}}\mathbf{b}^\star, (\bullet - \operatorname{mid}(\widehat{\mathcal{T}}))\operatorname{div}\widehat{\mathbf{q}_{\mathrm{RT}}})_{L^2(\Omega')} \lesssim \|h_{\mathcal{T}}(\mathbf{A}^{-1}\widehat{\mathbf{p}_{\mathrm{RT}}}^\star + u_{\mathrm{RT}}\mathbf{b}^\star)\|_{L^2(\Omega')}.$$

In conclusion of (i)–(iii), it follows that

$$R_2(\widehat{\mathbf{q}_{\mathrm{RT}}}) \lesssim \|h_{\mathcal{T}}\nabla_{\mathrm{NC}}\widehat{u_{\mathrm{CR}}}^\star\|_{L^2(\Omega')} + \|h_{\mathcal{T}}(\mathbf{A}^{-1}\widehat{\mathbf{p}_{\mathrm{RT}}}^\star + u_{\mathrm{RT}}\mathbf{b}^\star)\|_{L^2(\Omega')}. \tag{4.13}$$

On the other hand, the representation formula (4.5) shows that

$$\|h_{\mathcal{T}}(\mathbf{A}^{-1}\widehat{\mathbf{p}_{\mathrm{RT}}}^\star + u_{\mathrm{RT}}\mathbf{b}^\star - \nabla_{\mathrm{NC}}\widehat{u_{\mathrm{CR}}}^\star)\|_{L^2(\Omega')} = \|h_{\mathcal{T}}(\Pi_0 f - \gamma u_{\mathrm{RT}})\mathbf{A}^{-1}(\bullet - \operatorname{mid}(\mathcal{T}))\|_{L^2(\Omega')}.$$

With a lower bound $\underline{\varrho}$ of the smallest eigenvalue of A and with $\operatorname{div}\mathbf{p}_{\mathrm{RT}} = \Pi_0 f - \gamma u_{\mathrm{RT}}$ from (1.4),

$$\|h_{\mathcal{T}}(\mathbf{A}^{-1}\widehat{\mathbf{p}_{\mathrm{RT}}}^\star + u_{\mathrm{RT}}\mathbf{b}^\star - \nabla_{\mathrm{NC}}\widehat{u_{\mathrm{CR}}}^\star)\|_{L^2(\Omega')} \le \underline{\varrho}^{-1}\|h_{\mathcal{T}}^2\operatorname{div}\mathbf{p}_{\mathrm{RT}}\|_{L^2(\Omega')}.$$

For each $T \in \mathcal{T}$, $\|h_T\operatorname{div}\mathbf{p}_{\mathrm{RT}}\|_{L^2(T)} \approx \|(1-\Pi_0)\mathbf{p}_{\mathrm{RT}}\|_{L^2(T)}$ and an inverse estimate plus a uniform upper bound $\overline{\varrho}$ of the eigenvalues of $\mathbf{A}$ lead to

$$\begin{aligned}\overline{\varrho}\|h_{\mathcal{T}}^2\operatorname{div}\mathbf{p}_{\mathrm{RT}}\|_{L^2(T)} &\lesssim \overline{\varrho}\|h_{\mathcal{T}}(1-\Pi_0)(\mathbf{A}^{-1}\mathbf{p}_{\mathrm{RT}})\|_{L^2(T)}\\ &\le \|h_{\mathcal{T}}(1-\Pi_0)(\mathbf{A}^{-1}\mathbf{p}_{\mathrm{RT}})\|_{L^2(T)} \le \|h_{\mathcal{T}}(\mathbf{A}^{-1}\mathbf{p}_{\mathrm{RT}} + u_{\mathrm{RT}}\mathbf{b}^\star)\|_{L^2(T)}.\end{aligned}$$

The combination of the previously displayed estimates results in

$$\|h_{\mathcal{T}}(\mathbf{A}^{-1}\widehat{\mathbf{p}_{\mathrm{RT}}}^\star + u_{\mathrm{RT}}\mathbf{b}^\star - \nabla_{\mathrm{NC}}\widehat{u_{\mathrm{CR}}}^\star)\|_{L^2(\Omega')} \lesssim \|h_{\mathcal{T}}(\mathbf{A}^{-1}\mathbf{p}_{\mathrm{RT}} + u_{\mathrm{RT}}\mathbf{b}^\star)\|_{L^2(\Omega')}.$$

This and (4.13) plus some triangle inequalities imply

$$\begin{aligned}R_2(\widehat{\mathbf{q}_{\mathrm{RT}}}) &\lesssim \|h_{\mathcal{T}}(\mathbf{A}^{-1}\mathbf{p}_{\mathrm{RT}} + u_{\mathrm{RT}}\mathbf{b}^\star)\|_{L^2(\Omega')} + \|h_{\mathcal{T}}(\mathbf{A}^{-1}\widehat{\mathbf{p}_{\mathrm{RT}}}^\star + u_{\mathrm{RT}}\mathbf{b}^\star)\|_{L^2(\Omega')}\\ &\lesssim \|h_{\mathcal{T}}(\widehat{\mathbf{p}_{\mathrm{RT}}}^\star - \mathbf{p}_{\mathrm{RT}})\|_{L^2(\Omega')} + \|h_{\mathcal{T}}(\mathbf{A}^{-1}\mathbf{p}_{\mathrm{RT}} + u_{\mathrm{RT}}\mathbf{b}^\star)\|_{L^2(\Omega')}.\end{aligned}$$

Since $h_{\mathcal{T}} \le h_0 \lesssim 1$, this concludes the proof. □

Theorem 4.8 ((A3) Discrete Reliability). *Under the overall assumption that h_0 is sufficiently small, there exists some universal constant Λ_3, which depends on the global lower and upper bounds of the eigenvalues of $\mathbf{A}$ and on the universal stability constant of the discrete problems and on the shape-regularity in $\mathbb{T}$ such that the following holds. The discrete solutions $(\mathbf{p}_{\mathrm{RT}}, u_{\mathrm{RT}})$ and $(\widehat{\mathbf{p}_{\mathrm{RT}}}, \widehat{u_{\mathrm{RT}}})$ of (1.4) with respect to the triangulation $\mathcal{T}$ and its refinement $\widehat{\mathcal{T}}$ satisfy*

$$\Lambda_3^{-1}\delta^2(\mathcal{T},\widehat{\mathcal{T}}) \le \eta^2(\mathcal{T},\mathcal{T}\setminus\widehat{\mathcal{T}}) + \mu^2(\mathcal{T}) - \mu^2(\widehat{\mathcal{T}}).$$

Proof. This follows from the combination of Lemma 4.5, 4.6, and 4.7 with (4.9). □

Axiom (A3) implies the reliability result of [4, Theorem 5.5].

Corollary 4.9 (Reliability). *The solution* $(\mathbf{p}, u)$ *to* (1.3) *and the solution* $(\mathbf{p}_{\mathrm{RT}}, u_{\mathrm{RT}})$ *to* (1.4) *satisfy*

$$\|(\mathbf{p}-\mathbf{p}_{\mathrm{RT}}, u-u_{\mathrm{RT}})\|_{H(\mathrm{div},\Omega)\times L^2(\Omega)} \leq \Lambda_3^{\frac{1}{2}}\sigma(\mathcal{T}).$$

Proof. This follows from (A3) for a fixed triangulation $\mathcal{T}$ and a sequence of its successive uniform refinements $\widehat{\mathcal{T}}$ as then the maximal mesh-size in $\widehat{\mathcal{T}}$ tends to zero and standard estimates show convergence of $(\widehat{\mathbf{p}_{\mathrm{RT}}}, \widehat{u_{\mathrm{RT}}})$ to $(\mathbf{p}, u)$ in the norm of $H(\mathrm{div}, \Omega)\times L^2(\Omega)$. □

5 Verification of (A4)

The following lemma proves the supercloseness property (1.5) of $\Pi_0 u$ to the mixed solution u_{RT} with a duality argument. For given right-hand side $g \in L^2(\Omega)$, the dual problem seeks $\phi \in H_0^1(\Omega)$ with

$$\mathcal{L}^\star\,\phi := -\mathrm{div}(\mathbf{A}\nabla\phi) + \mathbf{b}\cdot\nabla\phi + \gamma\phi = g. \tag{5.1}$$

Under the overall assumption that $\mathcal{L}$ is injective, it follows that $\mathcal{L}$ and its dual $\mathcal{L}^\star$ are isomorphisms between $H_0^1(\Omega)$ and $H^{-1}(\Omega)$.

The reduced elliptic regularity of the leading elliptic part $-\mathrm{div}(\mathbf{A}\nabla\cdot)$ leads to higher regularity, that is, there exist α with $0<\alpha\leq 1$ and $C_{\mathrm{reg}}<\infty$ with

$$|\phi|_{H^{1+\alpha}(\Omega)} \leq C_{\mathrm{reg}}\|g\| \tag{5.2}$$

for any right-hand side $g \in L^2(\Omega)$ with the solution ϕ to (5.1) (see [12, Sections 5 and 14]).

The supercloseness (1.5) is discussed in the introduction and (unlike the remaining results of this paper) holds without any assumption on the initial mesh-size as long as (1.1) is injective and (1.4) has a solution.

Lemma 5.1 (Supercloseness). *The solution* $(\mathbf{p}, u)$ *to* (1.3) *and the solution* $(\mathbf{p}_{\mathrm{RT}}, u_{\mathrm{RT}})$ *to* (1.4) *satisfy* (1.5).

Proof. The dual problem (5.1) and its solution $\phi \in H_0^1(\Omega)\cap H^{1+\alpha}(\Omega)$ for the right-hand side $g = \Pi_0 u - u_{\mathrm{RT}} \in P_0(\mathcal{T})$ lead to $\mathbf{q} := \mathbf{A}\nabla\phi \in H(\mathrm{div},\Omega)\cap L^t(\Omega;\mathbb{R}^2)$ for some $t>2$. This allows the application of the Fortin interpolation operator I_F [3, pp. 107–109] with the commutative property $\Pi_0\,\mathrm{div}\,\mathbf{q} = \mathrm{div}\,I_F\mathbf{q}$. This and $\phi_h := \Pi_0\phi$ result in

$$\begin{aligned}\|g\|^2 &= -(g, \mathrm{div}\,\mathbf{q})_{L^2(\Omega)} + (g, \mathbf{b}\cdot\nabla\phi + \gamma\phi)_{L^2(\Omega)}\\ &= -(u-u_{\mathrm{RT}}, \mathrm{div}\,I_F\mathbf{q})_{L^2(\Omega)} + (g, \Pi_0(\mathbf{b}\cdot\nabla\phi) + \gamma\phi_h)_{L^2(\Omega)}.\end{aligned}$$

Equations (1.3)–(1.4) show $\Pi_0\,\mathrm{div}(\mathbf{p}-\mathbf{p}_{\mathrm{RT}}) = -\gamma g$ and

$$(u-u_{\mathrm{RT}}, \mathrm{div}\,I_F\mathbf{q})_{L^2(\Omega)} = (\mathbf{A}^{-1}(\mathbf{p}-\mathbf{p}_{\mathrm{RT}}) + (u-u_{\mathrm{RT}})\mathbf{b}^\star, I_F\mathbf{q})_{L^2(\Omega)}.$$

The combination of the aforementioned identities in the first step and the identity $\nabla\phi = \mathbf{A}^{-1}\mathbf{q}$ in the second step plus an integration by parts prove that

$$\begin{aligned}\|g\|^2 &= (\mathbf{A}^{-1}(\mathbf{p}-\mathbf{p}_{\mathrm{RT}}) + (u-u_{\mathrm{RT}})\mathbf{b}^\star, \mathbf{q}-I_F\mathbf{q})_{L^2(\Omega)}\\ &\quad + (\mathrm{div}(\mathbf{p}-\mathbf{p}_{\mathrm{RT}}), \phi-\phi_h)_{L^2(\Omega)} - (u-u_{\mathrm{RT}}, (1-\Pi_0)(\mathbf{b}\cdot\nabla\phi))_{L^2(\Omega)}.\end{aligned} \tag{5.3}$$

The error estimates of the Fortin interpolation plus piecewise Poincaré inequalities and the reduced elliptic regularity (5.2) of the dual problem (5.1) imply

$$\begin{aligned}\|\mathbf{q}-I_F\mathbf{q}\| &\lesssim h_{\max}^\alpha|\mathbf{q}|_{H^\alpha(\Omega)} \lesssim h_{\max}^\alpha\|g\|,\\ \|\nabla\phi - \Pi_0(\nabla\phi)\| &\lesssim h_{\max}^\alpha\|\phi\|_{H^{1+\alpha}(\Omega)} \lesssim h_{\max}^\alpha\|g\|,\\ \|\phi-\phi_h\| &\lesssim h_{\max}\|\nabla\phi\| \lesssim h_{\max}\|g\|.\end{aligned}$$

The application of these approximation properties to (5.3) concludes the proof. □

Recall that $\alpha > 0$ is the positive extra regularity parameter, which exclusively depends on the domain and on the coefficients, and the maximal initial mesh-size h_0 is the maximal mesh-size in $\mathcal{T}_0$ (whence in all $\mathcal{T} \in \mathbb{T}$) and Λ_3 is from (A3).

Theorem 5.2 ((A4$_\epsilon$) Quasi-Orthogonality). *There exists a constant $\Lambda_4' < \infty$ such that for sufficiently small h_0, any $\ell, m \in \mathbb{N}_0$ satisfy*

$$\Lambda_3^{-1} \sum_{k=\ell}^{\ell+m} \delta^2(\mathcal{T}_k, \mathcal{T}_{k+1}) \le 2\sigma_\ell^2 + \Lambda_4' h_0^{2\alpha} \sum_{k=\ell+1}^{\ell+m} \sigma_\ell^2.$$

Proof. Recall $\|\mathbf{p} - \mathbf{p}_\ell\|^2_{H(\mathrm{div},\Omega)} := \|\mathbf{A}^{-\frac{1}{2}}(\mathbf{p} - \mathbf{p}_\ell)\|^2 + \|\mathrm{div}(\mathbf{p} - \mathbf{p}_\ell)\|^2$ and abbreviate

$$e_\ell^2 := \|\mathbf{p} - \mathbf{p}_\ell\|^2_{H(\mathrm{div},\Omega)} + \|u - u_\ell\|^2 \quad \text{and} \quad \delta^2_{\ell,\ell+1} := \|\mathbf{p}_{\ell+1} - \mathbf{p}_\ell\|^2_{H(\mathrm{div},\Omega)} + \|u_{\ell+1} - u_\ell\|^2.$$

Elementary algebra plus (1.3)–(1.4) with respect to the triangulation $\mathcal{T}_{\ell+1}$, each with the test function $(\mathbf{p}_{\ell+1} - \mathbf{p}_\ell, u_{\ell+1} - u_\ell)$, eventually shows that $\delta^2_{\ell,\ell+1} + e^2_{\ell+1} - e^2_\ell$ is equal to

$$2\big(u - u_{\ell+1}, \mathbf{b}^\star \cdot (\mathbf{p}_{\ell+1} - \mathbf{p}_\ell) + (\gamma - 1)\,\mathrm{div}(\mathbf{p}_{\ell+1} - \mathbf{p}_\ell) - (u_{\ell+1} - u_\ell)\big)_{L^2(\Omega)}. \tag{5.4}$$

The factor $u - u_{\ell+1}$ in this L^2 scalar product is split into $\Pi_{\ell+1}u - u_{\ell+1}$ and $u - \Pi_{\ell+1}u$ with the L^2 projection $\Pi_{\ell+1}$ onto $P_0(\mathcal{T}_{\ell+1})$. Lemma 5.1 applies on the level of $\mathcal{T}_{\ell+1}$ and controls the L^2 norm

$$\|\Pi_{\ell+1}u - u_{\ell+1}\| \le C h_0^\alpha e_{\ell+1}.$$

This and the Cauchy inequality control the first contribution in (5.4) by $h_0^\alpha e_{\ell+1}\delta_{\ell,\ell+1}$ times the constant $2C(\|\mathbf{A}^{-\frac{1}{2}}\mathbf{b}\|^2_\infty + \|\gamma - 1\|^2_\infty + 1)^{\frac{1}{2}}$. The remaining second contribution in term (5.4) is the L^2 scalar product of $2(u - \Pi_{\ell+1}u)\mathbf{b}^\star$ with $(1 - \Pi_{\ell+1})(\mathbf{p}_{\ell+1} - \mathbf{p}_\ell)$ (recall that $\mathbf{b}^\star = \mathbf{A}^{-1}\mathbf{b}$ is a constant vector with length $|\mathbf{b}^\star| = \|\mathbf{b}^\star\|_\infty$). The Raviart–Thomas function $\mathbf{p}_{\ell+1} - \mathbf{p}_\ell \in RT_0(\mathcal{T}_{\ell+1})$ allows in 2D for

$$(1 - \Pi_{\ell+1})(\mathbf{p}_{\ell+1} - \mathbf{p}_\ell)(x) = \frac{1}{2}(x - \mathrm{mid}(T))\,\mathrm{div}(\mathbf{p}_{\ell+1} - \mathbf{p}_\ell)$$

at $x \in T \in \mathcal{T}_{\ell+1}$ and so

$$2\big((u - \Pi_{\ell+1}u)\mathbf{b}^\star, \mathbf{p}_{\ell+1} - \mathbf{p}_\ell\big)_{L^2(\Omega)} \le \frac{2}{3}|\mathbf{b}^\star| h_0 \|u - u_{\ell+1}\| \|\mathrm{div}(\mathbf{p}_{\ell+1} - \mathbf{p}_\ell)\| \le \frac{2}{3}|\mathbf{b}^\star| h_0 e_{\ell+1}\delta_{\ell,\ell+1}.$$

The combination of the two estimates for the two contributions in (5.4) leads (with $h_0 \le h_0^\alpha$ for $\alpha \le 1$ and $h_0 \le 1$) to

$$\Lambda_4' := \left(\frac{2}{3}\|\mathbf{b}^\star\|_\infty + 2C(\|\mathbf{A}^{-\frac{1}{2}}\mathbf{b}\|^2_\infty + \|\gamma - 1\|^2_\infty + 1)^{\frac{1}{2}}\right)^2$$

and

$$\delta^2_{\ell,\ell+1} + e^2_{\ell+1} - e^2_\ell \le h_0^\alpha (\Lambda_4')^{\frac{1}{2}} e_{\ell+1}\delta_{\ell,\ell+1} \le \frac{1}{2}\delta^2_{\ell,\ell+1} + \frac{1}{2}\Lambda_4' h_0^{2\alpha} e^2_{\ell+1}.$$

Provided that $\Lambda_4' h_0^{2\alpha} \le 2$, the sum of the above inequalities over different levels shows

$$\sum_{k=\ell}^{\ell+m} \delta^2_{k,k+1} \le 2e^2_\ell + \Lambda_4' h_0^{2\alpha} \sum_{k=\ell+1}^{\ell+m} e^2_k.$$

This and Corollary 4.9 with $e^2_k \le \Lambda_3 \sigma^2_k$ conclude the proof. □

Corollary 5.3 ((A4) Quasi-Orthogonality). *Axiom* (A4) *holds for sufficiently small initial mesh-sizes h_0.*

Proof. This follows from [8, Theorem 3.1] and (A4$_\epsilon$) for a sufficiently small $\epsilon := \Lambda_3\Lambda_4' h_0^{2\alpha} < \frac{1-\rho_{12}}{\Lambda_{12}}$ with parameters $0 < \rho_{12} < 1$ and $\Lambda_{12} > 0$ of the reduction result (A12) in [8, Theorem 4.1]. □

Remark 5.4 (Generalizations). Several arguments in this section apply to other mixed finite element methods as well but the second contribution in (5.4) solely applies to the Raviart–Thomas mixed finite element family. The restriction on the smallness of h_0 in Theorem 5.2 can be circumvented by the quasi-monotonicity (cf. [8] for the concept) but is required in Corollary 5.3.

6 Numerical Experiments

This section is devoted to numerical experiments to investigate the influence of the critical parameters h_0, θ_A, and κ and the practical performance of the adaptive algorithm SAFEM. After a few remarks on the implementation, three examples on the L-shaped domain are displayed with smooth or discontinuous right-hand sides, before some overall observations conclude the paper.

6.1 Numerical Realization

The *data approximation* is realized by the Thresholding Second Algorithm (TSA) of [1] followed by the closure algorithm to output a shape-regular triangulation.

Algorithm 2. TSA.

COMPUTE $\tilde{\mu}^2(T) = \mu^2(T)$ for all $T \in \mathcal{T}_0$ and set $\mu^2(\mathcal{T}_0) := \sum_{T\in\mathcal{T}_0} \mu^2(T)$.
SET $\mathcal{P} := \mathcal{T}_0$.

while $\mu^2(\mathcal{P}) >$ Tol **do**

  COMPUTE $\tilde{\mu}^2(T)$ for all $T \in \mathcal{P}$, set $\tilde{\mu}^2_{\max} := \max_{T\in\mathcal{P}} \tilde{\mu}^2(T)$.
  SELECT a subset $\mathcal{M} := \{T \in \mathcal{P} : \vartheta\tilde{\mu}^2_{\max} \le \tilde{\mu}^2(T)\} \subset \mathcal{P}$.
  COMPUTE $\overline{\mathcal{P}} := \texttt{bisec}(\mathcal{P}, \mathcal{M})$.

COMPUTE $\mathcal{T}_{\text{Tol}} := \texttt{completion}(\mathcal{P}) \in \mathbb{T}$.

The realization from [17, 18] is slightly modified in the APPROX algorithm of [1] through a parameter $\vartheta = 1 - 10^{-6} < 1$ in the computation of $\mathcal{M}$. The functional $\tilde{\mu}(T)$ in TSA is a weighted error functional, which depend on the values of $\mu(T)$ and $\tilde{\mu}(T)$ on the parent triangle T_P as well as on the siblings of T_P, cf. [1, 17, 18] for more details and the explicit formulas.

The *non-homogeneous boundary data* in Section 6.2 are not met in the theoretical part of this paper, which is simplified to homogeneous boundary conditions. The first example with known solution requires inhomogeneous boundary data on $\partial\Omega$ with the modified jump-term $(\mathbf{A}^{-1}\mathbf{p}_{\text{RT}} + u_{\text{RT}}\mathbf{b}^\star)|_E \cdot \tau_E + \frac{\partial u}{\partial s}|_E$ along the boundary edge $E \subset \partial\Omega$ with the prescribed boundary values u and its tangential derivative $\frac{\partial u}{\partial s}$ on E.

Short Notation. The abbreviation error ε (resp. estimator σ) refers to the left-(resp. right-)hand side of (2.1).

6.2 Continuous Right-Hand Side with Known Corner Singularity

The coefficients $\mathbf{A} = I$, $\mathbf{b} = (1, 1)$ and $\gamma = -2$ on the L-shaped domain $\Omega = (-1, 1)^2 \setminus [0, 1) \times (-1, 0]$ allow in (1.1) for a right-hand side f (computed by (1.1) for given u) and inhomogeneous Dirichlet boundary data (taken from u) for

$$u(r, \theta) = r^{\frac{2}{3}} \sin\Big(\frac{2\theta}{3}\Big)$$

in polar coordinates (r, θ) centered at the origin. The initial mesh $\mathcal{T}_0$ consists of 24 congruent right-isosceles triangles from a criss refinement of the three sub-squares and 28 degrees of freedom.

Figure 1 displays the outcome of SAFEM (Algorithm 1) with $\kappa = 1$, $\rho_B = \frac{1}{2}$, and various values of $\theta_A = 0.1$, 0.3, and 0.5. Despite the condition of Theorem 2.1 on the smallness of the bulk parameter θ_A, all displayed values result in an improved optimal empirical convergence rate $\frac{1}{2}$ compared to uniform mesh-refinement with a known suboptimal convergence rate $\frac{1}{3}$. The initial mesh is relatively coarse but all convergence rates are visible right from the beginning, the pre-asymptotic range is not visible. This examples allows the computation of the errors and the estimators and the equivalence is visible throughout with a the expected behavior.

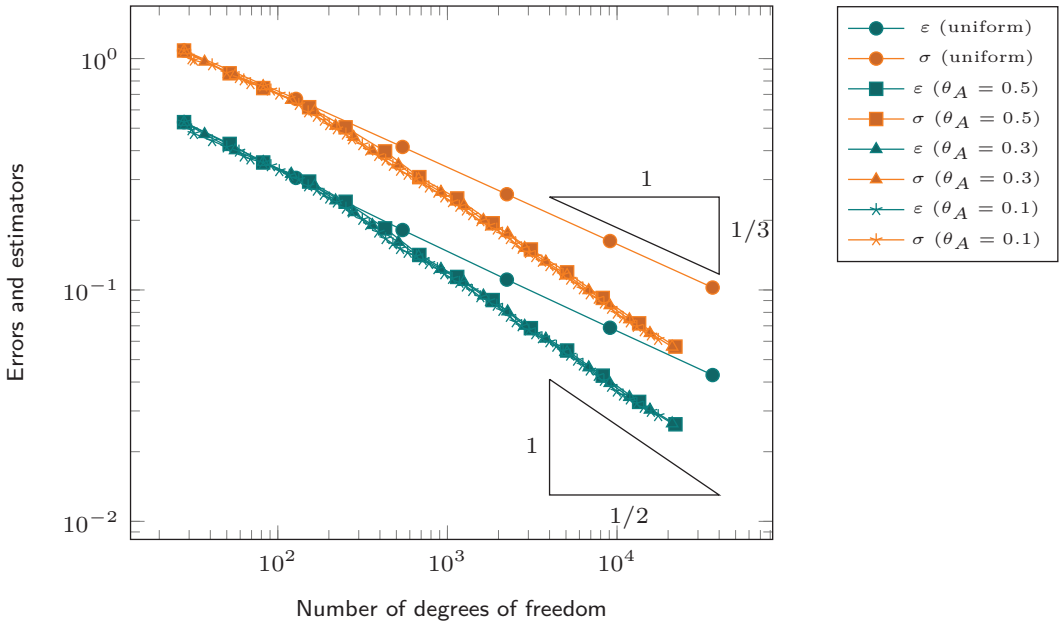

Figure 1: Convergence history plot for different values of θ_A in Section 6.2.

In the displayed experiment with $\kappa = 1$ only Case A of SAFEM applies as the right-hand side f is continuous. In case of $\kappa \leq 0.1$ for instance, only Case B runs in SAFEM for a very long computational range.

6.3 Constant Right-Hand Side

The coefficients $\mathbf{A} = 0.1I$, $\mathbf{b} = (1, 2)$ and $\gamma = -4$ on the L-shaped domain Ω with constant right-hand side $f \equiv 1$ lead in (1.1) to an unknown weak solution $u \in H^1_0(\Omega)$. Figure 2 (left) displays the output $\mathcal{T}_{13}$ of through SAFEM with $\kappa = 1$ and $\rho_B = \frac{1}{2} = \theta_A$. Besides the local mesh-refining at the re-entering corner, some layer of refinement are visible along some part of the boundary, that mimics a singular perturbed situation with $\mathbf{A} = \epsilon I$ for very small ϵ. Undisplayed numerical experiments for $\epsilon = 0.01$ have confirmed this observation even stronger.

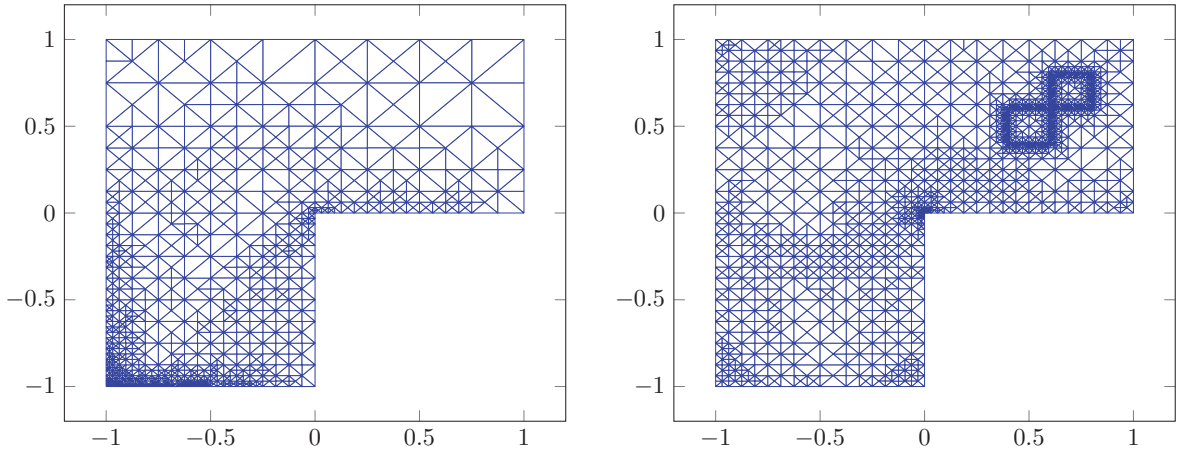

Figure 2: Triangulation $\mathcal{T}_{13}$ on level 13 in Section 6.3 with ndof = 2254 (left) and Section 6.4 with ndof = 4485 and $\epsilon = 1$ (right).

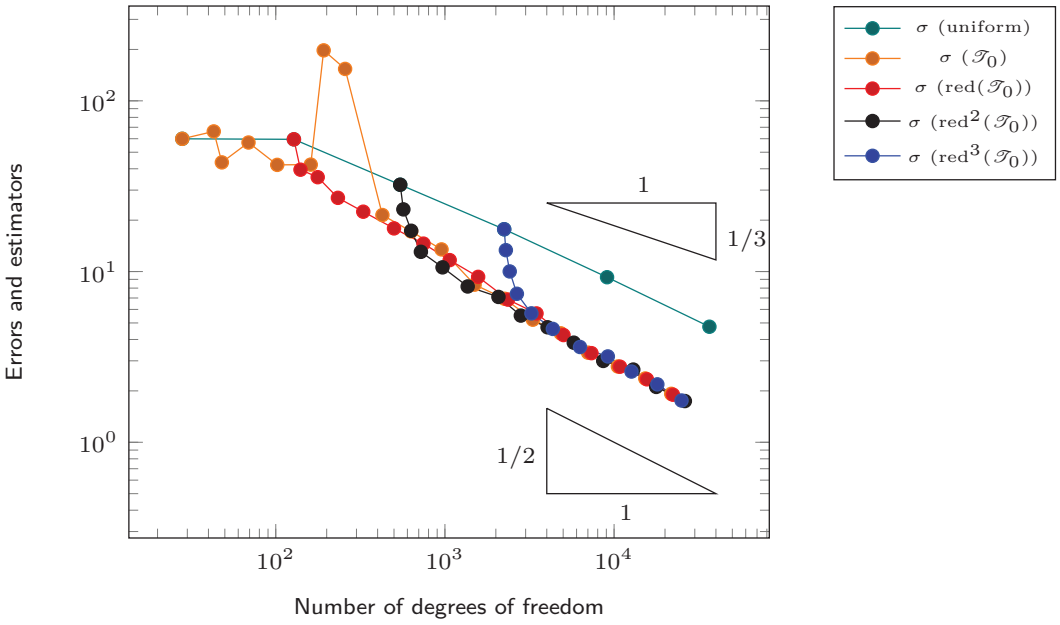

Figure 3: Convergence history plot for different initial input triangulations in SAFEM in Section 6.3 $\epsilon = 0.1$.

The convergence history plot of Figure 3 displays the estimators σ as functions of the number of degrees of freedom for various initial meshes, namely for $\mathcal{T}_0$ as described in the previous subsection and also for an initial mesh red($\mathcal{T}_0$) (of $\mathcal{T}_0$ from the previous subsection) with ndof = 140; red-refinement means the division of each triangle into four congruent sub-triangles by connecting its edges' midpoints with straight lines. This is plotted under the label σ(uniform) and shows the expected suboptimal empirical convergence rate. Those red-refined triangulations, e.g., red^2($\mathcal{T}_0$) (with ndof = 544) with two red-refinements and red^3($\mathcal{T}_0$) (with ndof = 2240) for three, serve as initial triangulations in the input of SAFEM and Figure 3 displays the respective convergence history plots.

The numerical experiment with the coarsest initial mesh $\mathcal{T}_0$ displays a pre-asymptotic range up to 1000 degrees of freedom. The finer initial triangulations lead to a much smaller pre-asymptotic range with a rapid decrease through a strong local mesh-refinement until the convergence rate of the other adaptive mesh-refinements is met. For the displayed parameter $\kappa = 1$, solely the Case A runs in SAFEM.

The undisplayed numerical experiment for a smaller parameter $\epsilon = 0.01$ leads to a much larger pre-asymptotic domain with a systematic error reduction only for a fine initial mesh red^3($\mathcal{T}_0$).

6.4 Piecewise Constant Right-Hand Side

Given the constant coefficients with $\mathbf{A} = \epsilon I$ and the domain as in the previous subsection, the right-hand side f for this example is piecewise constant with the values ± 1 and the value -1 exactly on the two squares $\omega := (\frac{2}{5}, \frac{3}{5})^2 \cup (\frac{3}{5}, \frac{4}{5})^2$ not aligned to the triangulations; $f|_{\Omega\setminus\omega} \equiv 1$ and $f|_\omega \equiv -1$. Figure 2 (right) displays the output $\mathcal{T}_{13}$ of SAFEM with $\kappa = 1 = \epsilon$ and $\rho_B = \frac{1}{2} = \theta_A$ with two squares ω visible by local mesh-refinements along $\partial\omega$ to resolve the discontinuity of the right-hand side f (recall that f is discontinuous at triangles that intersect $\partial\omega$). Cases A and B alternate in SAFEM for this example with $\epsilon = 1$ for the resolution of the discontinuities of the right-hand side at $\partial\omega$.

The convergence history plot for this example is not displayed as it looks very similar to that of the previous subsection (namely Figure 3) although the reasons for a larger pre-asymptotic range might be different.

For smaller values of ϵ, the triangulations look more like the picture in Figure 2 (left) from the previous subsection and solely Case A runs in SAFEM. Even for $\epsilon = 0.1$ (and more so for $\epsilon = 0.01$), the mesh-refinement displays boundary layers and no longer the discontinuities along $\partial\omega$.

6.5 Conclusions

The overall impression from the displayed and undisplayed numerical experiments is that the algorithm SAFEM is very robust such that the choice of θ_A, ρ_B, κ in the asymptotic convergence regime with an observed optimal convergence rate: The values $\theta_A = \frac{1}{2} = \rho_B$ and $\kappa = 1$ can be recommended throughout the examples of this paper. The condition on a sufficiently fine initial mesh $0 < h_0 \ll 1$ dramatically influences the pre-asymptotic behavior. Although the examples in Subsection 6.3 and 6.4 are very different in the right-hand side, the stability of the discrete system is identical. The finer the initial mesh, the smaller is the pre-asymptotic range in particular for $\mathbf{A} = \epsilon I$ with very small ϵ (e.g., $\epsilon = 0.01$). This paper exploits the situation when solely $\mathcal{L}$ is injective and then $0 < h_0 \ll 1$ appears necessary for the well-posedness of the discrete systems and has to be monitored in practise. It is conjectured that this dominates the difficulty of choosing an appropriate initial triangulation in SAFEM.

Acknowledgment: The work has been written, while the first author enjoyed the hospitality of the Hausdorff Research Institute of Mathematics in Bonn, Germany, during the Hausdorff Trimester Program *Multiscale Problems: Algorithms, Numerical Analysis and Computation*. The authors thank Rui Ma for a careful reading of the manuscript and her valuable remarks.

Funding: The research has been supported by the Deutsche Forschungsgemeinschaft in the Priority Program 1748 under the project Foundation and application of generalized mixed FEM towards nonlinear problems in solid mechanics (CA 151/22-1). The research was carried out while the second author (Asha K. Dond) enjoyed the support of the Priority Program 1748 *Reliable simulation techniques in solid mechanics. Development of non-standard discretization methods, mechanical and mathematical analysis* for a research visit at the Humboldt-Universität zu Berlin, Germany.

References

[1] P. Binev, W. Dahmen and R. DeVore, Adaptive finite element methods with convergence rates, *Numer. Math.* **97** (2004), no. 2, 219–268.
[2] P. Binev and R. DeVore, Fast computation in adaptive tree approximation, *Numer. Math.* **97** (2004), no. 2, 193–217.
[3] D. Boffi, F. Brezzi and M. Fortin, *Mixed Finite Element Methods and Applications*, Springer Ser. Comput. Math. 44, Springer, Heidelberg, 2013.
[4] C. Carstensen, A. K. Dond, N. Nataraj and A. K. Pani, Error analysis of nonconforming and mixed FEMs for second-order linear non-selfadjoint and indefinite elliptic problems, *Numer. Math.* **133** (2016), no. 3, 557–597.
[5] C. Carstensen, M. Feischl, M. Page and D. Praetorius, Axioms of adaptivity, *Comput. Math. Appl.* **67** (2014), no. 6, 1195–1253.
[6] C. Carstensen and R. H. W. Hoppe, Error reduction and convergence for an adaptive mixed finite element method, *Math. Comp.* **75** (2006), no. 255, 1033–1042.
[7] C. Carstensen and H. Rabus, An optimal adaptive mixed finite element method, *Math. Comp.* **80** (2011), no. 274, 649–667.
[8] C. Carstensen and H. Rabus, Axioms of adaptivity with separate marking for data resolution, *SIAM J. Numer. Anal.* **55** (2017), no. 6, 2644–2665.
[9] J. M. Cascon, C. Kreuzer, R. H. Nochetto and K. G. Siebert, Quasi-optimal convergence rate for an adaptive finite element method, *SIAM J. Numer. Anal.* **46** (2008), no. 5, 2524–2550.
[10] H. Chen, X. Xu and R. H. W. Hoppe, Convergence and quasi-optimality of adaptive nonconforming finite element methods for some nonsymmetric and indefinite problems, *Numer. Math.* **116** (2010), no. 3, 383–419.
[11] L. Chen, M. Holst and J. Xu, Convergence and optimality of adaptive mixed finite element methods, *Math. Comp.* **78** (2009), no. 265, 35–53.
[12] M. Dauge, *Elliptic Boundary Value Problems on Corner Domains. Smoothness and Asymptotics of Solutions*, Lecture Notes in Math. 1341, Springer, Berlin, 1988.
[13] A. K. Dond, N. Nataraj and A. K. Pani, Convergence of an adaptive lowest-order Raviart–Thomas element method for general second-order linear elliptic problems, *IMA J. Numer. Anal.* **37** (2017), no. 2, 832–860.
[14] W. Dörfler, A convergent adaptive algorithm for Poisson's equation, *SIAM J. Numer. Anal.* **33** (1996), no. 3, 1106–1124.

[15] M. Feischl, T. Führer and D. Praetorius, Adaptive FEM with optimal convergence rates for a certain class of nonsymmetric and possibly nonlinear problems, *SIAM J. Numer. Anal.* **52** (2014), no. 2, 601–625.
[16] K. Mekchay and R. H. Nochetto, Convergence of adaptive finite element methods for general second order linear elliptic PDEs, *SIAM J. Numer. Anal.* **43** (2005), no. 5, 1803–1827.
[17] H. Rabus, Quasi-optimal convergence of AFEM based on separate marking, Part I, *J. Numer. Math.* **23** (2015), no. 2, 137–156.
[18] H. Rabus, Quasi-optimal convergence of AFEM based on separate marking, Part II, *J. Numer. Math.* **23** (2015), no. 2, 157–174.
[19] L. R. Scott and S. Zhang, Finite element interpolation of nonsmooth functions satisfying boundary conditions, *Math. Comp.* **54** (1990), no. 190, 483–493.
[20] R. Stevenson, Optimality of a standard adaptive finite element method, *Found. Comput. Math.* **7** (2007), no. 2, 245–269.
[21] R. Stevenson, The completion of locally refined simplicial partitions created by bisection, *Math. Comp.* **77** (2008), no. 261, 227–241.